SLL 81 263/PB/M

LA-7715-MS

Informal Report

Anomalous Intense Driver (AID) Concept

University of California

LOS ALAMOS SCIENTIFIC LABORATORY
Post Office Box 1663 Los Alamos. New Mexico 87545

This report was not edited by the Technical Information staff.

UNITED STATES
DEPARTMENT OF ENERGY
CONTRACT W-7405-ENG. 36

Accession Number: 4090

Title: Anomalous Intense Driver (AID) Concept

Personal Author: Thode, L.E.

Corporate Author Or Publisher: Los Alamos Scientific Laboratory, PO Box 1663, Los Alamos, NM 87545
Report Number: LA-7715-MS

Report Prepared for: U.S. Department of Energy Report Number Assigned by Contract Monitor: SLL 81-263

Comments on Document: Archive, RRI, DEW. From Physical Review Letters

Descriptors, Keywords: Anomalous Intense Driver AID Concept Optimize Electron Bunch Mechanism Couple Energy Plasma Multikilovolt X-ray Source Inertial Confinement Thermonuclear Fusion

Pages: 54

Cataloged Date: Dec 10, 1992

Contract Number: W-7405-ENG.36

Document Type: HC

Number of Copies In Library: 000001

Record ID: 25650

Source of Document: DEW

ANOMALOUS INTENSE DRIVER (AID) CONCEPT

by

Lester E. Thode

ABSTRACT

An optimized electron bunching mechanism is utilized to efficiently couple the energy of a 5 to 100 MeV, 1 to 30 TW electron beam into a 3 to 50 cm^3 plasma of electron density 10^{17} to 10^{20} cm^{-3}. An efficient coupling of beam energy and momentum to the plasma is possible due to the relativistic nature of the beam dynamics combined with the short wavelength of the bunching mechanism in a high-density plasma. The rapidly produced multi-kilovolt plasma can be used directly to develop a pulsed neutron and x-ray source. Alternatively, the plasma can be used to drive a hierarchy of inertial confinement or x-ray devices. Utilizing this novel concept, controlled thermonuclear fusion may be achievable within present or near term relativistic electron beam technology.

I. INTRODUCTION

The Anomalous Intense Driver (AID) concept is an outgrowth of my investigations concerning the feasibility of heating a magnetically confined 10^{13} to 10^{17} cm^{-3} density plasma using an intense relativistic electron beam.[1-8] In the short term, the concept offers the potential for significant advancement in pulsed x-ray and neutron source technology, with materials studies, radiography, and weapons effects simulations as direct applications. Controlled thermonuclear fusion may also be achievable within present or near term relativistic electron beam technology. Central to the concept is the rapid heating of a 10^{17}-10^{20} electron cm^{-3}, 3 to 50 cm^3 volume of plasma by an intense, high-voltage relativistic electron beam. An efficient coupling is achieved through

the optimization and control of a very powerful collective wave interaction, which occurs naturally when a directed stream of electrons passes through a plasma.

Although the AID concept is based predominantly on theoretical calculations, the anomalous transfer of relativistic electron beam energy into both directed and thermal plasma energy has been observed experimentally.[7,9-13] As the mechanisms are nonclassical, a theoretical analysis of the coupling process is quite difficult, as the strength of the nonlinear state of the microinstabilities depends upon a large number of factors. Of course, the theoretical difficulty associated with the anomalous process is just a manifestation of the great versatility of the interaction, which is fully exploited within the AID concept.

The characteristic nonuniform energy deposition of the collective interaction is utilized to concentrate the energy in the plasma. In fact, the optimized relativistic electron beam-plasma interaction is a power density multiplication process. Since energy is being transferred from relativistic beam electrons to nonrelativistic electrons in the plasma, conservation of energy and momentum require that the interaction both heat and drive a localized axial current in the plasma. The driven axial current, in turn, generates an azimuthal magnetic field.

If the relativistic beam is solid, the physical configuration is similar to a nonuniform dense Z pinch in which the azimuthal magnetic field provides confinement. However, in contrast to a classical Z pinch, the heating and confinement are anomalous in character. For an annular relativistic electron beam, the azimuthal magnetic field leads to a directed heat flow towards the axis of the device. In this configuration, the kilovolt plasma can be used to drive a hierarchy of inertial confinement and x-ray devices.

Since the relativistic electron beam-plasma interaction has been studied extensively, both experimentally and theoretically, for approximately eight years, it is worthwhile to point out why the concept of an Anomalous Intense Driver has, to my knowledge, not been suggested previously. Basically, despite some initial encouraging results, lack of a consistent, definitive connection between experiment and theory, lack of theoretical techniques to investigate the interaction, and the programmatic dominance of CTR research combined to lead researchers away from an AID concept.

Historically, the investigation of the relativistic electron beam-plasma interaction appears to have been initiated in the Soviet Union in early 1970. Approximately twelve experiments,[7,9-13] which varied considerably in their complexity, have been carried out since that time. In fact, all experiments have reported an anomalous, or nonclassical, coupling of the beam energy to the plasma. The reported coupling has generally been attributed to

i) anomalous resistive heating due to the presence of a plasma return current (ion-acoustic and ion-cyclotron instabilities), and

ii) relaxation heating due to relativistic streaming instabilities (two-stream and upper-hybrid instabilities).

Early theory indicated that resistive heating[14] was a very efficient process for beams with $\nu/\gamma >> 1$. Here, ν/γ is a measure of the beam self-magnetic field energy to the beam particle energy. Defining N as the line density of beam electrons and r_e as the classical electron radius, $\nu \equiv Nr_e$ for a solid, constant density beam. The relativistic factor γ is related to the beam velocity v and speed of light c through the relationship $\gamma = [1-(v/c)^2]^{-\frac{1}{2}}$. The basic idea behind anomalous resistive heating is that a $\nu/\gamma >> 1$ beam cannot propagate since its self-magnetic field energy exceeds its particle energy. But, when such a beam is injected into a plasma, it neutralizes this characteristically large self-magnetic field energy by inducing a plasma return current. The relationship between the plasma and beam species in velocity space for a magnetically neutralized beam is shown in Fig. 1. Due to the relative drift between the plasma electron and ion species, ion-acoustic and/or ion-cyclotron waves are generated, as illustrated in Fig. 1 by the dashed lines. Such microturbulence is known to manifest itself as anomalous resistance. Thus, the plasma is heated at a rate

$$\frac{dW_p}{dt} = \eta^* J_p^2 \quad , \tag{1}$$

where W_p is the plasma energy density, η^* is the anomalous resistivity, and J_p is the plasma return current density. At the same time, the macroscopic electric field which maintains the return current, in order for the beam to propagate, removes energy from the beam. In this fashion, energy is transferred from the beam and deposited into plasma electrons and ions.

In contrast to resistive heating, relaxation heating results from the relative drift between the relativistic beam electrons and plasma electrons. Optimally, these instabilities take the form of electron bunching at a wavelength of

$$\lambda \cong (1\text{-}4)[10^{20}/n_e(cm^{-3})]^{\frac{1}{2}} \ \mu m \tag{2}$$

and a frequency of

$$f \cong [n_e(cm^{-3})/10^{16}]^{\frac{1}{2}} \ THz \ , \tag{3}$$

where n_e is the plasma electron density. The characteristic relationship between the plasma and beam species for optimized relaxation heating is illustrated in Fig. 2. Locally the net current I_{net} within the beam channel can exceed the beam current I_b, in contrast to the magnetically neutralized beam where $I_{net} \cong 0$ within the beam channel. As stated, this current multiplication is a consequence of momentum consevation, and is a very localized phenomenon. The location of the unstable spectrum for these instabilities is indicated by dashed lines in Fig. 2.

Early theory investigating relaxation heating was very crude,[1-3,14-26] and its applicability to experiments was seriously questioned. Moreover, different calculations varied dramatically in their predictions of the coupling efficiency. An extensive analysis[1,27] of the one-dimensional interaction was completed in 1973, which predicted that i) a maximum coupling efficiency of about 30% was possible, ii) most of the energy lost by the beam ended up in the plasma electrons, and iii) most of this energy took the form of high-energy electron tails. None of these characteristics were attractive for heating a magnetically confined plasma.

After a number of experiments had been carried out, it was generally observed that the coupling efficiency was approximately 15% when the plasma density was about 10^{12} electrons cm^{-3} but dropped rapidly to only a few percent as the density approached 10^{14} electrons cm^{-3}. This observed decrease in coupling efficiency as the plasma density increased was substantially more severe than predicted by the crude theory associated with streaming instabilities. As a result of these low observed efficiencies, coupled with the rather negative characteristics of relaxation heating theory, experimental attention

began to shift toward investigation of the resistive heating mechanism, which was considered to have properties compatable with the heating requirements of a CTR device.

The resistive heating mechanism has the ability to place a substantial fraction of the beam energy into plasma ions. This differs from the streaming instabilities which does primarily heat the plasma electrons. It was argued that the ions must be heated, and thus a mechanism which provides direct heating of the ions eliminates an energy conversion step. Furthermore, when energy is initially deposited into plasma electrons rather than the ions, heat conduction is enhanced due to the initially elevated electron temperature, so that achievable plasma confinement time is shortened. Consequently, increased external magnetic field strengths are required to produce comparable energy confinement.

The resistive heating mechanism also appeared to have the ability to heat a large volume of plasma in a uniform manner, rather than depositing energy in a small localized region, as is characteristic of the optimized streaming instability mechanism. The ability to heat directly a large volume of plasma in a uniform manner by resistive heating thus avoids problems of heat redistribution within the plasma. Moreover, the potential for developing a plasma heating system which could also be used in conjunction with devices requiring preheated plasmas and which, additionally, have high programmatic priority, such as tokamaks, rendered the resistive heating mechanism even more attractive. For these reasons, experimental investigations of the relativistic electron beam-plasma interaction in the United States were, in reality, motivated from the onset toward producing resistively heated plasmas. Consequently, experimental parameters to optimize resistive heating, such as low-voltage electrons beams with high v/γ outputs, were utilized in ongoing experiments. This evolution of the experiments is shown quite clearly in Figs. 3 and 4, which illustrate the decrease in maximum beam relativistic factor and increase in maximum v/γ for relativistic electron beam-plasma interaction experiments between 1970 and 1975.

Thus, the experiments virtually ignored any attempt to optimize the relaxation heating mechanisms, which, unknown to the experimentalists and theoreticians during the period 1970-1975, were being severly degraded by classical scattering of the relativistic electron beam as it passed through the anode foil. In so doing, experiments have clearly pointed out the limitations of

resistive heating, i.e., that resistive heating does not scale to higher density plasmas, but, to the contrary, is absolutely limited by self-stabilization within the plasma. More particularly, the experiments have shown that above a certain electron temperature, depending on the density of the plasma, low-frequency instabilities which are responsible for resistive heating, are stabilized. Consequently, only classical resistivity has any effect in resistively heating a high-density plasma.

As a result of these limitations, and the belief by most theoreticians and experimentalists that resistive heating dominated the anomalous energy deposition in a plasma, the relativistic electron beam-plasma heating program in the United States was virtually abolished in 1975 without any further investigation into the relaxation heating mechanism.

In early 1975 I developed a nonlinear theory for the streaming instabilities which took into account anode foil scattering,[28] the finite radial size of the plasma, and the strength of the external magnetic field. Subsequently, a comparison between the theory and all previous experimental data obtained for relativistic beam injection into preionized gas was carried out.[7] It was found that the scaling of the experimental heating data obtained by diamagnetic loops was in good agreement with the theoretical model. More importantly, it was apparent that the relativistic streaming instabilities in all previous experiments had been severely degraded at small beam-to-plasma particle density ratios due to excessive anode foil scattering.

These findings were first reported at a seminar I gave at Cornell University in May 1975. Subsequently, a limited experiment was carried out by Ekdahl et al.,[29] in which the thickness of the anode foil was varied for a fixed beam-to-plasma density ratio of 2.8×10^{-3}. The experimental results are compared with the theoretical scaling in Fig. 5. A factor of 4 to 5 increase in the coupling efficiency was achieved. Subsequently, a more detailed experiment was carried out at Cornell by Ekdahl and Sethian[30], in which both the anode foil thickness and beam-to-plasma density ratio were varied. These experimental results are compared with the theoretical scaling in Fig. 6. In this experiment a 350 keV electron beam was injected into a fully-ionized plasma of maximum density 6×10^{13} cm^{-3}. The maximum coupling efficiency at a beam-to-plasma particle density of approximately 3×10^{-3} was estimated to be 20 to 25%. Detailed numerical simulation indicates an optimized coupling efficiency near 60% for the basic experimental parameters. However, due to the low-voltage of the

beam, the degrading effect of foil scattering on the interaction was not overcome, as shown in Fig. 5. Also, the strength of the external magnetic field was nonoptimal.[31] Taking these two effects into account, the theoretical model predicts a coupling efficiency of about 25%. Thus, the observed magnitude and scaling of the heating are in very good agreement with theory. As a final point, although the deposition length was not directly measured, a distance of less than 20 cm is implied from other measurements.[32,33] Also, diamagnetic loop signals indicated the presence of a thermal wave.[34] Both observations are consistent with the theoretical picture.

In addition to the Cornell results, an unofficial comment[35] from the Novosibirsk group indicates a strong experimental dependence of the interaction strength on anode foil thickness. Using a 6 μm Ti foil, interactions which were highly localized near the diode were observed, with coupling efficiency exceeding 20%.

The significance of the Ekdahl and Sethian[30] experiment is the confirmation of the basic scaling of the relaxation heating process, although the observed large increase in coupling efficiency is, in itself, a major breakthrough. It follows, on the basis of the confirmed model, that to achieve an efficient coupling a high-voltage beam is required. This implies high-impedance, low ν/γ relativistic beam generator technology. Recall, this is the opposite direction taken by previous experiments. Moreover, the model indicates that high coupling efficiencies may be achievable at target plasma densities exceeding 10^{17} electrons cm^{-3}. In fact, as the plasma density is increased, the distance over which the beam deposits its energy becomes shorter and the wavelength of the bunching mechanism becomes small relative to the beam radial dimension. Both characteristics further imply the possibility of producing an intense, literally explosive plasma which was previously unattainable.

The potential of using a 5 to 100 MeV electron beam to anomalously deposit its energy into a 10^{17}-10^{20} electron cm^{-3} plasma was investigated theoretically during 1976. As reported in Ref. 36, such a beam would be capable of depositing its energy into a 2 to 10 centimeter long plasma target. Moreover, with careful generator design, a coupling efficiency of 15 to 50% could be achieved. For such a high coupling efficiency, local plasma energy densities of 10-50 kJ/cm^3 might be produced. To put this into context, high explosives can develop pressures as high as 15 kJ/cm^3. However, the time scale to develop such a

pressure is 10 to 100 times slower than the relativistic electron beam pulse. Thus, the power density associated with high-density, multi-kilovolt plasmas could exceed that of high explosives by over two orders of magnitude. Both present and near term conventional pulse power technology[37] and near term development of radial pulse line accelerators[38,39] appear suitable for this application. The time scale for the energy deposition is typically 50 to 150 ns for conventional pulse power technology, and 10 to 50 ns for the radial pulse line accelerator.

As a result of this analysis,[36] it was proposed to the Air Force Weapons Laboratory[40] that an experiment be carried out in the 10^{15}-10^{18} cm^{-3} regime to confirm the theory. As part of this experimental program, a preliminary propagation experiment recently carried out by Clark[41] provides further evidence of the strength of the interaction. In this experiment a 7 MeV beam was injected into a 43 cm long, 0.4 torr H_2 gas target. No external magnetic field was present. The beam energy transmitted to a calorimeter located 43 cm from the anode foil was measured as a function of the anode-cathode gap spacing and anode foil thickness. Anode foils of 25.4 μm kapton and 25.4 μm, 76.2 μm, 127.0 μm, and 304.8 μm titanium were used. Figure 7 shows a strong experimental dependence of the transmitted beam energy on the anode thickness and anode-cathode gap spacing. Ten centimeter long witness plates starting at the anode foil on the bottom of the gas container showed significant damage when the kapton foil was used, but showed little or no damage when the thicker titanium foils were used. The distortion of the anode foil was also found to depend dramatically upon foil thickness. Independent of foil thickness, the center region through which the beam passed is completely gone. However, the observed debris protrudes in the direction of beam propagation for the thicker titanium foils, while the kapton foil shows debris protruding in the opposite direction. Again, this is consistent with the formation of hot plasma in the vicinity of the foil, when a thin anode foil is used.

Although these results are preliminary, a not too unjustified conclusion is that a mechanism which depends upon the microscopic properties of the beam distribution function appears to severely disrupt beam propagation in a systematic fashion as foil scattering is reduced. Furthermore, the distance over which such a disruption occurs would appear to be about 5 to 10 cm with the kapton foil. (The classical range for a 7 MeV electron in 0.4 torr H_2 gas is

approximately 10^4 meter.) These obsevations, as well as the scaling with the anode-cathode gap, are consistent with the streaming instability.

In Sec. II a discussion of high-current relativistic electron beam generator and accelerator technology is given. This includes the cost, efficiency, and operational characteristics of present generator technology. A brief discussion of near term radial pulse line accelerator technology is also given. The AID concept is presented in Sec. III. Included are the anomalous pinch, fast liner, fast liner implosion of a microsphere, and x-ray generation configurations.

Alternate concepts for producing an intense pulsed x-ray or neutron source are discussed in Sec. IV. This section points out characteristic disadvantages of prior art concepts. Finally, a summary of the advantages the AID concept appears to have over prior art concepts is given in Sec. V.

II. RELATIVISTIC ELECTRON BEAM TECHNOLOGY

To practice the AID concept, a high-voltage, high-current density relativistic electron beam is required. Historically, high-voltage relativistic electron beam technology advanced rapidly during the 1960's, as shown in Fig. 8. This technology appears to have been developed predominantly by the Physics International Company for the Defense Nuclear Agency. Primarily, the generators were flash x-ray devices. Although this class of generator can deliver upwards of a megajoule in a 150 ns pulse, its characteristic high-impedance made it unattractive for driving very low-impedance devices. Thus, the strong development effort of this class of generator was abandoned in the early 1970's, in order to develop a low-impedance class of generators. This low-impedance class of generators is not appropriate for the AID concept.

To date, a number of high-impedance generators have been built. For example, the PI23-100, PI15-90, PI14-80, and PI9-50. Here, PI refers to the Physics International Company, the first number is the diameter of the Blumlein in feet, and the second number is the number of stages in the Marx generator. For the energy delivered, the generators are relatively compact in size; see Fig. 9. Also, the time to design and build such generators is relatively short. For example, the PI14-80 was recently designed and built in eight months.[37] As shown in Fig. 10, the cost of the technology is relatively inexpensive. A state of the art generator could produce a 16 to 20 MeV, 400 to 800 kA electron beam

with a pulse width of approximately 100 ns. The overall electrical efficiency for such a generator would be 40 to 45%. If the energy remaining in the Marx generator is recovered, the energy efficiency of such a generator would be 80 to 90%.

As shown in Fig. 11, high-impedance generators are composed of five basic components. A dc charging system is used to charge the Marx generator, which is the primary energy storage component. The Marx generator consists of a large number of stages which are charged in parallel and discharged in series using spark gap switches. A typical Marx stage consists of two capacitors connected in series with a center ground to allow positive and negative dc charging; see Fig. 12a.

The Marx generator is then used to charge a Blumlein. A Blumlein is essentially two coaxial transmission lines connected in series with the diode impedance Z_D; see Fig. 12b. Physically, the Blumlein appears as three concentric, annular conductors. This folded configuration is used to reduce the spatial dimension of the Blumlein. In operation, the center conductor is charged through an inductor L_c which appears as a short. Once charged, the switch S_o connecting the center and intermediate conductors is closed, and the inner transmission line begins to discharge with a pulse propagating toward the diode. When the pulse hits the impedance discontinuity, a voltage appears across the diode. As opposed to the shorted inner transmission line, which has an impedance Z_I, the outer transmission line, with impedance Z_0, is open. Thus, for a properly matched configuration ($Z_0 = Z_I = Z_D/2$) a voltage equal to charge voltage on the inner conductor appears across the diode for a period twice the propagation time down the transmission line. The inductor L_c appears as an open circuit during the Blumlein discharge. For high voltages the Blumlein uses transformer oil as a dielectric.

Due to the physical configuration of the Blumlein, it is difficult to design the inner and outer transmission lines such than $Z_I = Z_0$. Thus, there is typically a very small, but noneligible, voltage that appears across the diode during the Blumlein charge. From the standpoint of proper operation of a high-current density diode, this so-called prepulse must be suppressed. Significant progress in prepulse suppression has occurred in the past few years. Through the use of prepulse switches combined with careful design of the feed and diode region, a prepulse of less than 50 kV has been demonstrated for a 9 MV Blumlein charge.[37] With this advance in prepulse suppression beam particle

densities exceeding 10^{14} cm^{-3} have been obtained in a focused flow configuration.

Physically, the Blumlein output is connected to a feed which transmits the pulse to the diode. The feed usually radially converges the pulse, and thus also transforms its voltage and impedance.

The final component is the diode, which can be either foil or foilless for the AID concept. Foil diodes appear to suffer rapid impedance collapse when the current density exceeds 20 kA/cm^2. Presently, this effect is not clearly understood. It appears, however, that the physics of this problem has not been considered in a systematic fashion and that obtaining current densities up to 100 kA/cm^2 is possible with improved vacuum systems. Note that this is predominantly a basic physics problem, as opposed to improvements in generator technology. Foilless diodes appear naturally suited for the AID concept when the plasma is utilized to drive power multiplication and x-ray devices. However, the operation and flow characteristics of such diodes could be significantly advanced. In fact, initial investigation[43] of the foilless diode indicates that current densities of up to 1 MA/cm^2 are possible.

Pulsed high-current electron beams with particle energy exceeding 20 MeV can be produced with a radial pulse line accelerator.[38,39] Basically, this is a linear accelerator with radial transmission or Blumleins providing energy to the accelerating gaps. Radial lines are composed of coaxial disk or cone conductors, and thus can be stacked in series. As a result, the accelerator is amenable to mass production, probably at a cost of less than $5/joule delivered. In addition, the development time for a 200 to 800 kJ, 5 to 20 TW, 10 to 100 cycle per second prototype accelerator is less than five years. The injector for such an accelerator could be the high-current generator discussed previously, or the first accelerating stage. A conceptional diagram of the radial pulse line accelerator is shown in Fig. 13. Pavlovskii and coworkers[38] claimed to have constructed such an accelerator. The accelerator is also being studied by Humphries.[44]

Multi-megajoule electron beams might be produced using explosive magnetic flux driven generators[45] as the primary source of energy. In fact, the use of such generators to drive a transmission line has received detailed investitation.[46] Utilizing fuses to increase the delivered voltage of such devices, beam powers of 100 TW appear possible.

III. DESCRIPTION OF AID CONCEPT

A. Discussion of Anomalous Interaction

In the past all devices or concepts directed towards producing neutrons or x-rays via fusion seem to be classical in character. For example, CTR magnetic confinement research has attempted from its inception to minimize the collective character of the plasma. If collective effects have been considered, they generally have been invoked in hopes of overcoming some detrimental aspect of a particular concept. For example, anomalous absorption of hot electrons generated at the critical surface during the absorption of laser light has been considered.

The essential new idea in the AID concept is to take advantage of two extremely powerful microinstabilities.[2] As a result, large scale technology development efforts are bypassed. The source of these instabilities is the relative drift between a relativistic electron beam and plasma electrons. In its optimized form, these streaming instabilities are electron bunching mechanisms. In the past, devices based upon electron bunching, for example, klystons and magnetrons, have resulted in significant technology advances. Such devices, however, generally only operate efficiently under proper conditions. This characteristic is also true for the electron bunching mechanisms utilized in the AID concept.

Determining conditions for which the streaming instabilities are optimal is difficult due to the large number of independent factors which can influence the interaction. Some aspects of the interaction have been analyzed in detail while others have only been subjected to a cursory analysis. Some of the analysis has been written up in detail,[1-9,27-28,31,36,40,43] but most of the last eighteen months work has not. This includes approximately two-hundred hours (CDC 7600) of fully relativistic, electromagnetic, cylindrical injection computer simulations, hybrid calculations, hydrodynamic code calculations of laser produced target plasmas, and hydrodynamic code calculations of explosive plasma driven devices. Some of the unpublished work is presently being used to design experiments at the Air Force Weapons Laboratory.[40] It is inappropriate to attempt a detailed discussion of the nonlinear theory in the present paper. However, a very brief summary of my investigations follows.

1. Optimal Coupling Coefficient.

The basic dependence between the beam relativistic factor $\gamma = (1-\beta^2)^{-\frac{1}{2}}$, beam particle density n_b, and plasma electron particle density n_e is given by

the strength parameter[4] $S = \beta^2\gamma(n_b/2n_e)^{1/3}$. The potentially large coupling efficiency associated with the relativistic streaming instabilities is a consequence of the relativistic dynamics, the strength of which depends upon S. Specifically, if an electron undergos a change in velocity $\delta\beta = \delta v/c$, its change in energy is $\delta\gamma = \gamma^3\beta\delta\beta/(1 + \gamma^2\beta\delta\beta)$. For the streaming instabilities, the characteristic change in velocity incurred during bunching is $\delta\beta \cong \gamma^{-1}(n_b/2n_e)^{1/3}\beta$. It follows that

$$\delta\gamma/\gamma \cong \gamma^2\beta\delta\beta/(1 + \gamma^2\beta\delta\beta) = S/(1 + S) \quad ,$$

which can be of order unity.

More detailed analysis indicates that not all the beam electrons act coherently during the bunching process, since their individual responses vary with energy. Basically, this is phase mixing. Denoting α as the coupling coefficient, a one-dimensional analysis yields[9]

$$\alpha = 1.5\ S(1+1.5\ S)^{-5/2} \quad , \tag{6}$$

which maximizes at $S \cong 0.45$ with $\alpha \cong 0.19$. This rather pessimistic result is still believed to be correct by the great majority in the plasma physics community.

In reality, the assumption that the nonlinear state is one-dimensional is physically incorrect for an optimized interaction. Since the relativistic electron beam will relax strongly in both energy and angle, it is necessary to carry out a self-consistent, two-dimensional, fully relativistic nonlinear calculation to determine the coupling coefficient. Such calculations can only be carried out using advanced particle code techniques.[47] Because such codes are expensive to run and cannot be employed for all physical parameter regimes of interest, an analytical procedure or model has been developed which determines the magnitude of various parameters for optimal interactions.[36] Based upon this model and extensive numerical particle simulations, an optimal coupling efficiency of

$$\alpha_{optimal} \cong S/(1 + S) \tag{7}$$

appears achievable. In fact, simulations demonstrating a kinetic energy coupling exceeding 60% have been carried out.[31]

2. Factors Influencing Coupling Coefficient.

Over the past four years considerable progress has been made in understanding the nonlinear evolution of the two-stream and upper-hybrid instabilities. The dependence of the interaction on the following have been considered:

1) beam relativistic factor,[1-9]
2) beam particle density,[1-9]
3) plasma particle density,[1-9]
4) anode foil scattering,[7,9,28,36]
5) larmor radius effects resulting from radially dependent ordered transverse motion,[36]
6) wavelength of instability relative to radial size of the beam and plasma,[36]
7) radial plasma gradients,[36]
8) externally applied magnetic field strength,[2,6,31,36]
9) plasma temperature,[36]
10) electron-ion and electron-neutral collision rate,[9]
11) ionization state of plasma and ionization gradients,
12) plasma hydrodynamic gradients,
13) beam pinching resulting from current multiplication,
14) premodulation, and
15) time dependence of the electron beam power.

It has been found that the electron random motion or temperature along a streamline and the wavelength of the instabilities relative to the radial size of the plasma primarily determines the ability of the interaction to sustain a high coupling efficiency over the entire beam pulse.

Beam temperature along a streamline can result from the random motion associated with the temperature of the cathode surface. However, transverse temperatures of 300-1000 eV at the emission surface are required before this source of random motion begins to degrade the interaction. Due to the high-voltage applied to the cathode, electrons are field emitted with typical transverse energies of 1 to 20 eV. Thus, this source of random motion is negligible.

A possibly more serious source of random motion is electron emission from the cathode shank and lack of beam equilibrium at the emission surface. However, by shaping the cathode and anode surfaces properly, and by simultaneously

applying an external magnetic field to the diode region, this source of random motion can also be reduced to a negligible level.

In fact, beam temperature along a streamline seems to result primarily from the passage of relativistic electrons through thin foils. Extensive analysis has shown that the effect of such a foil on the interaction can be made negligible. The effect of a foil is to reduce the fraction of beam electrons $\Delta n/n_b$ which can act coherently during the development of the instability, with

$$\frac{\Delta n}{n_b} = 1 - \exp(-S/F) \ . \tag{8}$$

Typical values for the foil scattering function[9,36] F are given in Table I. It follows that increasing γ and decreasing the foil's effective thickness results in the factor exp(-S/F) approaching zero. Thus, the beam can penetrate a closed container and retain a high coupling efficiency to the enclosed target plasma.

TABLE I

FOIL SCATTERING FUNCTION F BASED UPON MOLIÈRE THEORY OF MULTIPLE SCATTERING. THE SCATTERING ANGLE IS APPROXIMATELY $\theta \cong F^{\frac{1}{2}}/\beta^2\gamma$

x(μm)	127.0	254.0	508.0	762.0	1270.0	2540.0
Deuterium Tritium 50/50	0.00447	0.0114	0.0276	0.0455	0.0843	0.191

x(μm)	12.7	25.4	50.8	76.2	127.0	254.0
Mylar	0.0111	0.0292	0.0716	0.119	0.221	0.504
Kapton	0.0115	0.0300	0.0735	0.122	0.227	0.517
Beryllium	0.00944	0.0245	0.0597	0.0987	0.183	0.417
Graphite	0.0211	0.0526	0.125	0.205	0.378	0.852
Aluminum	0.0541	0.132	0.310	0.505	0.924	2.07
Titanium	0.168	0.397	0.913	1.47	2.67	5.91

It has generally been argued that the transverse motion associated with the beam self-fields is an effective temperature. If no external magnetic field

is present and the beam is injected into a plasma in order to obtain equilibrium, such ordered motion can evolve into random motion. However, for the optimized interaction, the coherence length of the beam is long relative to the deposition length. Thus, high-voltage, low v/γ beams in a focused flow configuration can interact strongly with a plasma, provided the plasma begins at the anode foil and $\Delta n/n_b \cong 1$. This has been confirmed by numerical simulation and is supported by the Clark experiment.[41]

If the target plasma is also high-density, the wavelength associated with the streaming instabilities is very short compared with the radial dimensions of the beam and plasma; see Eq. (2). Under these conditions, the optimal nonlinear evolution of the instability is highly two-dimensional, and once initiated is extremely difficult to degrade. Beam pinching due to the formation of plasma hydrodynamic gradients and due to current multiplication can result in the instantaneous deposition rate varying in time. Such a time variation is not monotonic, however.

3. Deposition Length.

The distance over which the relativistic electron beam can deposit upwards of $S/(1 + S)$ of its kinetic energy is

$$L_N \cong 10\ \gamma(n_e/n_b)^{1/3}\ c/\omega_p\ , \tag{9}$$

where ω_p is the target plasma frequency and c is the speed of light. This is orders-of-magnitude shorter than classical range of megavolt electrons in 10^{17}-10^{20} cm^{-3} density plasma. For example, if $n_b(\gamma)$ is determined from a one-dimensional, relativistic diode result,[48]

$$L_N \cong \Gamma(\gamma)(d^2/M)^{1/3}\ cm\ . \tag{10}$$

In Eq. (10) the diode gap spacing is d and the adiabatic compression ratio is M. The dimensionless parameter $\Gamma(\gamma)$ is shown for given values of the plasma electron density n_e in Fig. 14. Because waves e-fold from noise most of the beam energy is actually deposited over a length shorter than L_N by a factor of 2 to 3. The characteristic nonuniform energy deposition of the collective mechanisms, two-stream and upper-hybrid instabilities, is shown in Fig. 15, for both the one- and two-dimensional interactions. In the AID concept, this nonuniform deposition property is utilized to concentrate energy deposited into

the plasma from the relativistic electron beam, rather than allowing the energy to dissipate its explosive character by expansion into a much larger volume of plasma.

B. Discussion of Components and Operation

Two basic approaches for utilizing a relativistic electron beam driven, high-energy density plasma to produce radiation and neutrons are envisioned.

First, a direct use of the plasma as the source by confining its energy for a sufficient length of time. In this approach a solid relativistic electron beam penetrates a 3 to 50 cm^3 gas filled container, and transfers a fraction of its energy and momentum to the enclosed gas. Conservation of energy and momentum requires that the beam both heat the plasma and drive a large axial plasma current. The presence of the large axial current, in turn, initiates additional ion heating and confinement. This configuration is similar to a dense Z-pinch. At high plasma density the option for predominantly heating electrons or heating both electrons and ions exists. This is possible because the classical equipartition time between the plasma species and electron heating rate can be varied significantly. Figure 16 is a conceptual diagram illustrating the major components of a device which uses the high-energy density plasma as a source.

Alternatively, an annular relativistic electron beam is utilized to penetrate a 3 to 50 cm^3 gas filled container, and transfers a fraction of its energy and momentum to the enclosed gas. Again conservation of energy and momentum requires the beam both heat the plasma and drive a large axial plasma current. However, the heated plasma is annular, and the large axial current leads to directed heat flow towards the interior of the annular region, where devices which are engulfed and driven by hot electrons are located. Such devices can take the form of power multiplers, which might be cylindrical, spherical, or ellipsoidal in shape. By adjusting the electron heating rate and plasma density, the options of driving such devices by ablation or exploding pusher exit. Also, control of the driving electron temperature and distribution is possible by varying the plasma density and magnitude of the external magnetic field. Soft x-ray devices can be obtained by allowing the hot plasma to heat moderate to high Z wire arrays, for example. A conceptual diagram of the major components of a system to utilize a high-energy density plasma to drive power multiplication or x-ray conversion devices is shown in Fig. 17.

Many modifications and variations of the configurations shown in Figs. 16 and 17 are possible. For example, early applications of the concept would not require the use of a low-density gas chamber 52, modulator 38, drift tube and adiabatic compressor 36, or the radial pulse line accelerator 32. With advances in relativistic electron beam technology the external magnetic field 70, preionizers 62 and 64, and windows 54, 56, 58, and 60 might not be necessary. With annular beams, multiple beam systems are possible, as depicted in Figs. 18 through 20. For multiple beam systems, the energy deposition regions do not overlap, and thus such systems are intended to drive larger devices.

1. Relativistic Electron Beam Generator and Accelerator.

The relativistic electron beam generator 30 produces a solid 34 or annular 35 high-voltage, high-current density relativistic electron beam. A solid beam can be produced using a foil diode. If a plasma is not in contact with the anode foil, a mesh screen of high optical transparency could replace the foil. Annular beams can be produced using a foil, screen, or foilless diode. Within present technology, diode voltages of 15 to 20 MV are possible. Using the generator 30 as an injector to a radial pulse line accelerator 32, a high current beam with electron energy in the 100 MeV range appears realistic.

2. Vacuum Drift Tube and Adiabatic Compressor.

The relativistic electron beam 34 or 35 propagates along the vacuum drift tube and adiabatic compressor 36 to the modulator 38. An external solenoidal magnetic field source 40 generates a magnetic field in the generator diode, accelerator, drift tube, and modulator regions to ensure a laminar flow beam equilibrium. In the vacuum drift tube 36, the strength of the external magnetic field can be increased along the direction of beam propagation to produce adiabatic beam compression. Modest compression ratios can reduce the beam radius a factor of 2 to 3, while preserving a laminar flow equilibrium, provided the compression is carried out in vacuum.[43] A vacuum system 42 maintains the required vacuum.

3. Modulator.

Modulator 38 constitutes an inner portion of the vacuum drift tube and is formed by a periodic structure or dielectric along the direction of beam propagation. A rippled magnetic field could also be used to parametrically modulate the beam. The purpose of the modulator 38 is to provide an enhanced narrow band fluctuation level (very weak modulation) at a wavelength and phase velocity

slightly below the natural wavelength and phase velocity of the instability in the target plasma 68 or 72.

The underlying idea behind this weak modulation is increased coupling efficiency. For waves propagating along the relativistic electron beam axis, the characteristic growth rate δ/ω_p and characteristic change in beam velocity $\delta\beta = 2(\beta - \omega/k)$ for the streaming instability as a function of the wave number $k = 2\pi/\lambda$ are shown in Fig. 21. Here ω/k is the phase velocity associated with the electrostatic spectrum, and v is the initial beam velocity. The growth rate is normalized to the plasma frequency ω_p. For an unmodulated beam the nonlinear evolution of the streaming instability is determined by the fastest growing wave, which occurs at $kv/\omega_p = 1.1$ in this example. The beam energy loss is thus determined by

$$\delta\gamma/\gamma \cong \gamma^2\beta\ \delta\beta(\text{unmodulated})/[1 + \gamma^2\beta\ \delta\beta(\text{unmodulated})] = \chi S/(1 + \chi S) \quad , \quad (11)$$

as described previously. However, by enhancing the noise level at a wavelength and phase velocity slightly shorter and slightly lower than the fastest growing wave, the beam energy loss is determined by $\delta\beta$(modulated) shown in Fig. 21. The coupling efficiency is then increased to

$$\delta\gamma/\gamma \cong \gamma^2\beta\ \delta\beta(\text{modulated})/[1 + \gamma^2\beta\ \delta\beta(\text{modulated})] = \chi S/(1 + \chi S) \quad , \quad (12)$$

where $\chi \cong 1.0$ to 1.3 based upon preliminary analysis of the modulated interaction. Physically, the modulation leads to an enhanced strength parameter. Thus, the modulation also reduces the effect of foil scattering and collisions on the interaction.

4. Low-Density Gas Chamber, Isolation Foil, and Initiation Foil.

The low-density gas chamber 52 provides isolation between the replaceable target plasma container 66 and modulator 38, drift tube and adiabatic compressor 36, accelerator 32, and generator 30. The electron density in the ionized low-density plasma channel 46 is typically close to the relativistic electron beam density, whereas the target plasma electron density is 4 to 6 orders of magnitude above the beam density. The low-density gas 50 might be H_2, He, Ar, N_2 or residual gas associated with the previous operation of the system.

Foil 44 provides isolation between the vacuum modulator 38 and the low-density plasma channel 46, and converts a small fraction of the rising beam impulse into Bremsstrahlung radiation which is directed predominantly along the direction of beam propagation. The isolation function is provided by layer of metal (titanium, aluminum, or beryllium), graphite, or plastic, such as mylar (C_{10} H_8 O_4), kapton (C_{22} H_{10} N_2 O_5), or polycarbonate. A layer of plastic impregnated with high Z atoms, a fine mesh high Z wire screen with a very high optical transparency, or a high Z aperturing layer[47] could be used to provide the Bremsstrahlung radiation. Such Bremsstrahlung radiation would aid in the creation of the low-density plasma channel 46 for beam propagation through the low-density gas 50. With advances in beam technology, foil 44 could be replaced by differential pumping of the modulator 38.

Foil 48, which provides isolation between the low-density plasma channel 46 and the dense target plasma 68 or 72 is constructed in a similar fashion to foil 44. It also acts to initiate the collective interaction and generate Bremsstrahlung radiation for partial ionization of the dense plasma target 68 or 72, to assist or replace preionizers 62 and 64.

In the ionized low-density plasma channel 46 and target plasma 68 or 72, the self-fields of the beam are shorted out so that an external magnetic field is not required to achieve beam equilibrium. Subject to more extensive analysis, the beam might be ballistically guided through the low-density plasma channel 46 to the plasma target 68 or 72. However, the overall efficiency of the system would be enhanced by the presence of an external magnetic field source 70. Also, the external magnetic field source 70 can provide increased stabilization of the relativistic electron beam within the low-density plasma channel 46.

5. Preionizers.

Preionizers 62 and 64 provide full ionization of the target plasma 68 or 72. Any number of devices for creating a fully-ionized gas such as a discharge tube, channel forming wire, various lasers (including free-electron lasers), plasma gun, microwave generator, or low-energy particle beam could be used. It appears, however, that the laser might be the best device for creating a low-temperature, fully-ionized plasma in the 10^{17} to 10^{20} cm^{-3} density range.

With a laser preionizer, windows 54, 56, 58, and 60 formed from sapphire, salt, or other appropriate materials would be positioned in the low-density gas chamber 52 and target plasma container 66. For a fully-ionized target density

of 8×10^{18} to 10^{20} electrons/cm^3 a 0.1 to 2.0 μs, 0.2 to 10kJ HF laser, or a number of smaller HF lasers, would be used as preionizers 62 and 64. A 0.1 to 2.0 μs, 0.2 to 3kJ CO_2 laser, or a number of smaller CO_2 lasers, would be appropriate for fully-ionized density less than 8×10^{18} electrons/cm^3.

Based upon analysis which is not fully self-consistent, the combination of Bremsstrahlung radiation via foil 48, direct impact collisions, avalanche, and the initial collective interaction can fully ionize the target plasma 68 or 72. However, the beam requirements are more stringent when the relativistic beam provides both ionization and heating of the target plasma 68 or 72. Thus, use of preionizers 62 and 64 lowers the relativistic electron beam technology requirements.

6. Anomalous Pinch.

The anomalous pinch is the simplest mode of operation within the AID concept. The relativistic electron beam target is a simple gas filled container. As a neutron source the anomalous pinch intrinsically requires a plasma density greater than 10^{19} cm^{-3}. As a result, the relativistic electron beam, laser, and external magnetic field requirements push the state of the art, and technologically this mode of operation is the most difficult to achieve. The target gas would be DT or DD.

As an alternative approach to a pulsed neutron source, the anomalous pinch could be operated as a target for intense deuterium beam generated by the rapidly developing pulse power light-ion beam technology.[50-54] Operating with a plasma density of approximately 10^{18} cm^{-3}, the plasma electron temperature can be elevated sufficiently to reduce the cross section for deuterium beam energy absorbsion by target plasma electrons.[55] Thus, the probability of survival of energetic trapped deuterium ions to undergo fusion with the plasma deuterium and tritium ions is significantly enhanced. Although this two component concept is an old one, intense neutron pulses could be produced using present pulse power technology.

A moderate Z gas or a mixture of H_2 and high Z gas with an electron density of 10^{17}-10^{19} cm^{-3} could be used for the target plasma 68 to produce x-rays. In the radiation mode, beryllium windows in the target plasma container 66 would be provided, and the low-density gas chamber 52 may not be present. Such a tunable x-ray source would be suitable for a variety of applications.

In operation, the relativistic electron beam 34, Fig. 16, penetrates foil 48 and convective wave growth is initiated such that the waves e-fold until

saturated through nonlinear trapping of the beam electrons. Since the nonlinear waves are not normal plasma modes, they are absorbed into the plasma very rapidly through nonlinear mode beating. Actually, this nonlinear mode beating acts throughout the entire interaction and keeps the level of electric field energy relatively low compared with the energy transferred from the beam to the plasma. The presence of the foil 48 thus ensures that the beam energy is deposited at a specified location within the target plasma container 66, as opposed to moving upstream.

Since energy and momentum are being transferred from relativistic electrons 34 to nonrelativistic electrons within the target plasma 68, the beam both heats the target plasma and drives an axial current in it. The presence of the axial current, in turn, initiates ion heating and plasma energy confinement. Taking into account increased internal pressure resulting from the non-ohmic process, an equilibrium pinch configuration is formed with currents in the multi-megampere range, with significant reduction in heat conduction losses. Relative to the typical classical Z-pinch, the development of the anomalous pinch would be much faster.

For a solid relativistic electron beam, the anomalously generated azimuthal magnetic field 69 and heated plasma column 67 is illustrated in Fig. 22. The axial nonuniformity in the azimuthal magnetic field 69 strength is similiar to the energy deposition, Fig. 15. Primary energy loss out of the anomalous pinch is indicated by arrows. The presence of an external axial magnetic field and proximity of the radial wall both tend to provide stable operation.

7. Laser Preionization Configurations

Figure 23 is a schematic illustration of one possible arrangement for the anomalous pinch. As shown, relativistic electron beam generator 30 produces a solid relativistic beam 34 which is propagated through the vacuum tube and adiabatic compressor 36 and adjacent modulator 38. The relativistic electron beam 34 then penetrates foil 44, passes through the low-density plasma channel 46, penetrates foil 48, and anomalously transfers a fraction of its energy and momentum to the target plasma 68 thereby forming the anomalous pinch. Windows 76 and 78 allow the laser ionization beam 82 to penetrate the target plasma container 66 and low-density gas chamber 52. A salt or sapphire window would be appropriate for a CO_2 or HF laser, respectively. An ionization beam intensity of 10^9 to 10^{11} watts/cm^2 would be used.

Hydrodynamic code calculations indicate that a fully-ionized plasma with sufficient axial uniformity can be formed using the configuration shown in Fig. 23. The laser energy is transferred to the target plasma through inverse Bremsstrahlung. Consequently, the target plasma exhibits a slightly decreasing gradient along the direct of propagation of the relativistic electron beam 34. Such a decreasing gradient actually tends to increase the strength of the deposition, since its effect on the nonlinear dynamics is similiar to premodulation. In fact, the ability of the streaming instabilities to counteract self-consistent plasma hydrodynamic gradients is related to this dynamical effect.

Figure 24 is an alternative arrangement in which two lasers 92 and 94 apply ionization beams 96 and 98 transverse to the axis of the relativistic electron beam 34. Windows 84 and 90 in the low-density gas chamber 52 structure and windows 86 and 88 in the target plasma container 66 structure allow passage of the ionization beams to the target plasma 68.

Figure 25 is a schematic end view of an additional alternative arrangement utilizing three lasers 112 through 116 which produce ionization beams 118 through 122. Windows 106 and 110 in the low-density gas chamber 52 structure and windows 100 through 104 in the target plasma container structure 66 provide ionization beams 118 through 122 access to the target plasma 68. The advantage of the arrangement shown in Fig. 25 is that lasers 112 through 116 can be arranged in an off-axis position such that their beams are not directed at each other.

Although the single laser beam configuration shown in Fig. 23 will produce the desired target plasma, additional magnetic field energy would be required to deflect the residual relativistic electron beam. Also, the cost and technology associated with a single large laser is greater than with a number of smaller lasers with the same combined energy. Thus, the multiple laser configurations shown in Figs. 24 and 25 would seem to be superior.

The preceding laser configurations also are appropriate for systems which use the high-energy density plasma to drive power multiplication or x-ray conversion devices, as shown in Fig. 17. Since the laser intensity is quite low, the hot electron spectrum generated by such a beam interacting directly with a power multiplication device would be negligible. Also, except for the radial profiles of the relativistic electron beam, the major components and operation are idential in Figs. 16 and 17 up to the target plasma container 66. Thus,

only the target plasma container and its interior operation will be discussed further.

8. Fast Liners

Historically, high explosives or magnetically driven thin, cylindrical metallic shells have been referred to as liners. These are hybrid devices in that they incorporate concepts common to both magnetic and inertial confinement of plasma. Liners have been used to compress magnetic fields,[56] compress and heat magnetically confined plasma,[56,57] and generate x-rays.[58] Within the AID concept, this type of power multiplication device can be generalized to include spherical and ellipsoidal shapes. Since the liners will be multilayer in design, they might equally well be thought of as pellets.

Initially, there was some question concerning the utility of a high-density, multi-kilovolt plasma beyond the obvious application as an x-ray source. Consequently, utilizing the anomalous coupling theory to describe the energy source, the author carried out a number of hydrodynamic code calculations which considered ablatively driven flat plates by high-density, multi-kilovolt plasma. These, admittedly crude, calculations indicate that implosion velocities exceeding 10^7 cm/sec could be obtained using present relativistic electron beam technology. Moreover, these implosion velocities are achieved on the time scale of the relativistic electron beam pulse length.

A configuration suitable for driving fast spherical or cylindrical liners is shown in Figs. 26 and 27. Here a single laser ionization beam 126 entering through window 124 is used. Multiple laser ionization configurations as shown in Figs. 24 and 25 can also be used. Recall that the use of lasers for pre-ionization appears, on the basis of preliminary analysis, to lower the relativistic electron beam technology requirements. Thus, subject to additional theoretical and experimental investigation, the laser ionization sources should be considered as optional.

An annular relativistic electron beam 35 penetrates the initiation foil 48, which also acts as an end plug. As the voltage and current density rise, the anomalous coupling coefficient increases to its optimal value, and the beam transfers a large fraction of its energy and momentum to the annular plasma region 73. The beam driven azimuthal magnetic field 75 in turn directs the annular plasma 73 thermal energy to the fast spherical 125 or cylindrical 128 liner. Since the source of the azimuthal magnetic field 75 is the result of an axial current flow in the annular plasma 73, resulting from conservation of

momentum, it is not present in the vicinity of the fast spherical 125 or cylindrical 128 liner. The presence of an axial external magnetic field generated by 70 can be used to increase the anomalous coupling coefficient. However, as the annular plasma column 73 and plasma engulfing the liner are very high beta, this field is partially excluded.

The radial wall of the plasma target container 66 is sufficiently thick to ensure magnetic flux containment and sufficiently massive to provide radial inertial confinement (tamper) on the relativistic electron beam time scale. Thus, radial energy loss to the container wall is limited by both the azimuthal magnetic field 75 and partially excluded external magnetic field. Heat conduction is limited axially on the beam time scale by the lower axial temperature gradient, azimuthal magnetic field 75, and self-mirroring of the external magnetic field. Thus, the geometry takes advantage of anomalous coupling and classical heat conduction to rapidly and efficiently remove energy from the relativistic electron beam 35 and transport it to the fast liner.

A cross-sectional view of the basic configuration with dual laser ionization beams 134 and 136 is shown in Figs. 28 and 29. Here windows 130 and 132 are placed in the radial wall of the plasma container 66.

Detail of the fast spherical 125 and cylindrical 128 liner is shown in Figs. 30 and 31. The fast liner consists of an ablator 144 or 150, pusher 146 or 152, and solid buffer 148 or 154. The ablator is boiled off through heat conduction, with the pusher and solid buffer propelled to high implosion velocity. Since the thermal conductivity of a plasma is a strong function of temperature, the rate at which energy is transported to the liner increases in time throughout the beam pulse. Thus, some natural shaping of the plasma driving source is obtained. Such shaping can lead to stronger compression and heating[59,60] of the gas fuel 138 or 142.

Structured spherical pellets similiar to the liner 125 have been studied extensively with respect to laser implosion.[59-62] The ablator 144 or 150 is a low Z, low mass density material such as LiDT, Be, ND_3BT_3, boron hydride, or CDT. Pusher 140 or 152 is typically a higher Z and mass density material such as glass, aluminum, gold, or nickel. It could also be plastic embedded with high Z atoms. Solid DT or LiDT could be used for the solid buffer 148 or 154. Depending upon the implosion velocity desired and stability considerations, the total mass of the fast liner 125 or 128 would be 1 to 500 milligrams.

In the case of the cylindrical liner 128, shaping would minimize loss of the enclosed fuel 142 out the ends, as shown in Fig. 31. Alternatively, the ends could be plugged if it proved advantageous for the annular plasma 73 and fuel 142 to be different. An ellipsoidal shaped liner could also be used.

A configuration similiar to the LASL CTR Division's magnetically driven fast liner[57] concept is illustrated in Fig. 32. Here a solid beam penetrates foil 160 and forms an anomalous pinch 158 within the cylindrical liner 128, which is driven by an annular beam entering through foil 48. Deflector 156 provides for initial ionization in the anomalous pinch region 158.

A target geometry, utilizing two annular relativistic electron beams to drive a spherical liner 125 is depicted in Fig. 33. The operation of configuration is essentially the same as discussed previously. Care must be taken to minimize the beam deflection as it passes through the respective beam driven azimuthal magnetic field regions, as indicated in Fig. 18.

9. Fast Liner Implosion of Structured Microspheres. An alternate approach towards obtaining an intense neutron source is to use the high-density, multi-kilovolt relativistic electron beam produced plasma to drive a fast liner, which then produces an intense, shaped energy pulse suitable for imploding structured microspheres.[59-62] Such microspheres would be filled with DT, DD, DHe^3, HLi^6, or HB^{11}, for example.

The following four paragraphs describing the fast liner are essentially identical to the description given in the preceding discussion.

The basic geometry of this approach is shown in Figs. 34 and 35, for a single laser ionization beam 126 entering through window 124. The multiple laser ionization configurations as shown in Figs. 24 and 25 can also be used. Recall that the use of lasers for preionization appears, on the basis of preliminary analysis, to lower the relativistic electron beam technology requirements. Thus, subject to additional theoretical and experimental investigation, the laser ionization sources should be considered as optional.

An annular relativistic electron beam 35 penetrates the initiation foil 48, which also acts as an end plug. As the voltage and current density rise, the anomalous coupling coefficient increases to its optimal value, and the beam transfers a large function of its energy and momentum to the annular plasma region 73. The beam driven azimuthal magnetic field 75 in turn directs the annular plasma 73 thermal energy to the fast spherical 125 or cylindrical 128 liner. Since the source of the azimuthal magnetic field 75 is the result of an

axial current flow in the annular plasma 73, resulting from conservation of momentum, it is not present in the vicinity of the fast spherical 125 or cylindrical 128 liner. The presence of an axial external magnetic field generated by 70 can be used to increase the anomalous coupling coefficient. However, as the annular plasma column 73 and plasma engulfing the liner are very high beta, this field is partially excluded.

The radial wall of the plasma target container 66 is sufficiently thick to ensure magnetic flux containment and sufficiently massive to provide radial inertial confinement (tamper) on the relativistic electron beam time scale. Thus, radial energy loss to the container wall is limited by both the azimuthal magnetic field 75 and partially excluded external magnetic field. Heat conduction is limited axially on the beam time scale by the lower axial temperature gradient, azimuthal magnetic field 75, and self-mirroring of the external magnetic field. Thus, the geometry takes advantage of anomalous coupling and classical heat conduction to rapidly and efficiently remove energy from the relativistic electron beam 35 and to transport it to the fast liner.

The fast liner consists of an ablator 144 or 150, pusher 146 or 152, and solid buffer 148 or 154, see Figs. 36 and 37. The ablator is boiled off through heat conduction, with the pusher and solid buffer propelled to high implosion velocity. The ablator 144 or 150 is a low Z, low mass density material such as LiDT, Be, ND_3BT_3, boron hydride, or CDT. Pusher 146 or 152 is typically a higher Z and mass density material such as glass, aluminum, gold, or nickel. It could also be plastic embedded with high Z atoms. Solid DT or LiDT could be used for the solid buffer 148 or 154. Depending upon the implosion velocity desired and stability considerations, the total mass of the fast liner 125 on 128 would be 1 to 500 milligrams.

The gas buffer 172 could be DT or DD, for example. In the case of the cylindrical liner 128, the ends could be plugged if it proved advantageous for the annular plasma 73 and gas buffer 182 to be different. Alternately, the fast liner could be ellipsoidal in shape. For closed liners, the buffer gas could be a moderate Z gas.

As the liner collapses, the density and temperature of the buffer gas 172 in contact with the microsphere 170 increases in time. Such pulse shaping, which would be different for the cylinder and sphere, allows shock overtaking[59,60] producing high compression of the ablative driven microsphere 170.

Using the high-density thermal gas 172 or 182 for implosion reduces the preheating problem associated with the microsphere 170.

Basic detail of the microsphere 170 is shown in Figs. 36 and 37. The materials used for the ablator 174, pusher 176, solid buffer 178, and gas fuel 180 would be similiar to those proposed previously.[59-62] Of course, the final design in terms of size and layer thickness will differ for the liner-microsphere combination since the driving source is now a high-density, multi-kilovolt plasma. It is clear that multiple pusher configurations utilizing velocity multiplication to obtain very high implosion velocity can also be used in the microsphere 170.

10. X-Ray Generation. A variety of x-ray generation devices can be envisioned, the geometry depending upon the specific application. Basically, high Z material of various sizes and shapes are engulfed and rapidly heated by high-density, multi-kilovolt plasma. The spectrum and rate of radiation is controlled by changing the total mass, Z, and opacity of the device.

As an example, Figs. 38 and 39 show a soft x-ray source in which a wire array is engulfed by the high-density, multi-kilovolt plasma 73 produced by an annular relativistic electron beam 35. The device could be directly attached to the drift tube or modulator 194.

The target plasma container 66 is a simple cylinder which is lined with a high Z material 186. A beryllium window 190 is provided for radiation extraction. A wire array 188 is supported by the initiation foil 184 and end plug 192. The size, shape, and number of wires in the array 188 depends upon the opacity of the materials. Wires of aluminum, titanium, tantalum, tungsten, or stainless steel with diameters of 5 to 100 μm appear suitable. Such an array is designed to have a low opacity in the direction of the beryllium window 190.

Due to the compact size and directional properties of the above device it would appear possible to operate it as a module in a configuration producing multi-megajoule level radiation output with a 10 to 100 ns pulse length.

IV. PRIOR ART CONCEPTS

A. Relativistic Electron Beam Magnetically Confined Plasma Heating

In this prior art concept the relativistic electron beam is required to heat a large volume of plasma to thermonuclear temperature, which is then contained by an elaborate magnetic field configuration. As a result, the relativistic beam is relegated to a relatively minor role, and thus its intrinsic

high efficiency is of little consequence to the overall efficiency of the system. In addition, the beam energy is required to be deposited in a rather slow and uniform fashion in this prior art application. Since the optimal anomalous beam deposition is naturally rapid and nonuniform, the beam interaction is limited and its explosive character dissipated by expansion into the large volume plasma. In other words, the dimensions of the plasma are much larger than the characteristic deposition length of the optimal anomalous process and no attempt is made to utilize the plasma's explosive character. Due to the large volume of plasma to be heated to thermonuclear temperature, the total energy stored in the beam is considerably beyond present technology. Since the initial deposition is into plasma electrons, rather than ions, this is seen as a disadvantage in the prior art concept in which the ions must ultimately be heated. It also follows that heat conduction, which limits the energy containment time, is enhanced due to the initially elevated electron temperature. In general, heat conduction is a limiting process in the prior art concept. Finally, since the relativistic beam is only secondary to the overall system, the versatility associated with the optimal anomalous process is reduced to a single application with respect to simulation and fusion, primarily by limiting the plasma density to less than 10^{17} cm^{-3} due to magnetic confinement limitations.

A typical configuration of a prior art experimental apparatus is shown in Fig. 40. A cathode 196 is positioned within a vacuum chamber 198 which is separated from the plasma chamber 200 by an anode foil 202. A series of dielectric spacers are separated by a series of metal plates 204 which function to prevent breakdown between the cathode 196 and the diode support structure 206. A solenoidal or mirror magnetic field configuration 208 is produced by an external source along the axial direction of the device.

In operation, a relativistic electron beam 210 is formed by charging the cathode 196 with a fast risetime voltage pulse, causing electrons to be emitted from the cathode 196 penetrating the anode foil 202 so as to enter the plasma chamber 200 as a relativistic electron beam 210. As the relativistic beam propagates through the plasma along the externally applied magnetic field 208, the beam couples its energy to the plasma 212 in an anomalous fashion.

B. Laser Magnetically Confined Plasma Heating

In this concept a laser, rather than a relativistic electron beam, is used to heat to thermonuclear temperature a large volume plasma, which is again

confined by an elaborate magnetic field system. As with the electron beam, the laser plays only a secondary role in the system. Although a laser does provide uniform ionization and rapid heating of a low temperature plasma, the characteristic deposition length increases approximately as $T^{3/2}$ for a plasma electron temperature T above 10 eV. This character of the deposition coupled with the large volume of plasma to be heated places a total energy requirement for the laser which are one to two orders of magnitude larger than present technology can provide. Even if such lasers could be developed, the inherent low efficiencies associated with lasers would result in a large capital investment in such a system.

C. Ion Beam Magnetically Confined Plasma Heating

A similar system incorporates a light- or heavy-ion beam to deposit its energy in a magnetically confined plasma. Since such beams are nonrelativistic, they exhibit a very low coupling efficiency and lack versatility obtainable by the relativistic interaction.

D. Dense Z-Pinch

In this prior art concept the Z-pinch plasma is part of an electrical circuit, and, as such, the electrodes connecting the plasma to the external circuit are subject to damage. In addition, circuit inductance has limitied the current rise time, although recently it has been proposed that this limitation might be overcome by driving the Z-pinch with a 100-200 kV transmission line.[63] Since the radius of the pinch is typically small relative to its length, the pinch is susceptable to a number of hydrodynamic instabilities. Also, the Z-pinch is purely classical and thus limited in the number of independent parameters.

E. Fast Liners

In the prior art concept fast liners are driven by magnetic forces. The liners can be used to heat and confine a plasma for neutron[56,57] production or can undergo self-collision for x-ray production.[58]

For this prior art concept, the liner is basically part of an electrical circuit. Thus, the external circuit resistance and finite liner resistivity lead to ohmic looses, which lowers the efficiency of converting electrical energy into liner kinetic energy. Since the liner must make electrical contact with the remainder of the circuit, connecting electrode, 220 and 222 in Fig. 41, damage can be severe and the system again falls into a basic single shot character. Also in Fig. 41, the prior art initial liner geometry 224 is

typically cylindrical, which limits compression and power multiplication relative to a spherical implosion.

Due to ohmic heating, implosion velocities exceeding 10 cm/μs can be achieved only if the liner is initially a thin foil, which is converted into a plasma. Although this colliding plasma concept acts as an efficient x-ray source (an annular beam could also drive a liner to produce x-rays in this fashion), the foil plasma cannot be considered as a massive pusher capable of efficiently compresssing a plasma. Also, the liner is converted into a plasma, the thickness of the liner is increased, which lowers the potential for power multiplication. Even with very thin foils, implosion velocities are limited by the risetime of the driving current and the diffusion of the driving magnetic field through the plasma liner.

If the liner is to remain a solid conducting shell (massive pusher) ohmic heating and magnetic field diffusion limits implosion velocities to 1-3 cm/μs. For such low implosion velocities, the plasma must be preionized (not shock heated). Due to the long implosion time heat conduction losses must be overcome, leading to embedding magnetic field requirements in the prepared plasma.[57] Plasma requirements, with respect to initial temperature and density, also appear difficult.

F. Inertial Confinement

Basically, this concept involves the compression of a pellet by a laser, electron beam, light-ion beam, or heavy-ion beam. In the prior art concept, the target and driving source are directly coupling through primarily classical interactions. Thus, direct preheat of the fuel by the driving source represents a major problem in the direct coupling concept. As such, the characteristics of the target and driving source are closely coupled, which leads to large scale development programs for the required sources.

The main disadvantages of the laser is its low efficiency and associated high-development cost. Preheat by hot electrons produced at the critical surface also appears to limit target design and performance.

Low-impedance electron beam and light-ion beam sources appear to be limited by propagation of the beam to the pellet. For electron beams the fuel is preheated by bremsstralung. Focusing the beams to millimeter diameters also poses a formidable problem. Technology advancement is required to obtain the power level necessary for compression, with development costs similar to that of the laser.

Heavy-ion sources require significant technological advancement and appear to be a factor of two to five times more expensive than lasers. There is also some question concerning the stable propagation of such a beam to the target.

V. SUMMARY

To begin, it is worthwhile to point out a fundamental difference between laser and relativistic electron beam deposition in a plasma. Since laser light absorption below the critical frequency takes place through classical inverse bremsstrahlung, the energy is initially deposited near the plasma suface. Thus, only after the plasma surface has been heated does the laser begin to deposit its energy into the interior of the plasma. In contrast, a relativistic electron beam deposits its energy anomalously, and thus the characteristic deposition length remains essentially invarient as the plasma electron temperature increases. The relativistic electron beam energy is predominantly deposited into the interior of the plasma, relatively far removed from the plasma surface and container walls.

In principle a light- or heavy-ion beam could be used to deposit their energy in an anomalous fashion in a plasma. However, such beam are nonrelativistic, and, as a result, exhibit a very low coupling efficiency and a lack of versatility relative to the relativistic interaction. It follows that the concept of an Anomalous Intense Driver is achievable only through intense high-voltage relativistic electron beam technology.

The concept of an Anomalous Intense Driver depends upon the literally explosive heating of a 10^{17} - 10^{20} cm^{-3} plasma. Since the relativistic electron beam provides the bulk of the energy to drive the system, full advantage of the beam's high efficiency is utilized. In contrast to prior art, the volume of the heated plasma is small (3 to 50 cm^3) and high density (10^{17} - 10^{20} cm^{-3}). Short time plasma particle confinement results from a combination of i) azimuthal magnetic fields generated during the anomalous interaction and ii) inertial and self-mirroring associated with the external magnetic field. The external magnetic field also serves to optimize the electron bunching mechanism.

The nonuniform deposition shown in Fig. 15, characteristic of the anomalous mechanism, is utilized to concentrate the deposited energy, rather than allowing it to dissipate its explosive character by expansion into a large volume plasma. The initial deposition into plasma electrons, rather than ions,

and heat conduction are both used to the advantage of the device, rather than being disadvantages in the prior art.

Due to the high-coupling efficiency, any technology advances, if required, would be modest. Also, the cost to obtain the required relativistic electron beam is modest, relative to other sources, due to its high efficiency and advanced technology.

Depending upon the density of the plasma to be heated, a CO_2 or HF laser is utilized to produce a uniform plasma. The laser is required only to heat the plasma slightly to reduce the initial collision rate. Thus, the laser is being used in an efficient manner, relative to the prior art laser heating concept. As a result, the laser requirements are within present or near term technology.

Within the framework of the AID concept, four classes of devices are proposed: i) Anomalous Pinch, ii) Fast Cylindrical or Spherical Liner iii) Fast Liner Implosion of a Microsphere and iv) Soft X-ray Wire Array.

The anomalous deposition can produce a significant enhancement in the local plasma current. This current enhancement, which has been observed in both simulations and experiment, is the result of an exchange in momentum between relativistic and nonrelativistic electrons. Conservation of momentum predicts that the current enhancement is inversely proportional to the v/γ of the beam. It follows that local currents of 1-10 MA, with risetimes of approximately 100 ns, can be driven in the plasma by the beam.

In addition to driving a plasma current, the beam heats the plasma. Taking into account this increased pressure resulting from the nonohmic process, an equilibrium pinch could be formed for currents in the 5-10 MA range. The development of such a pinch using a solid beam could lead to ignition in a simple and straightforward manner. Relative to the prior art, this technique for producing a dense pinch allows for a faster rise in the current and significant nonohmic heating. The larger equilibrium pinch current leads to a larger self-magnetic field, which is expected to reduce heat conduction. Also, since the beam is propagated to the inertially confined plasma, electrode damage considerations are overcome. As a result, the concept loses its single shot character by utilizing a small replaceable gas filled container.

If the beam is annular, the intense plasma generated by the anomalous coupling can be used drive fast cylindrical liners. In this concept heat conduction rapidly transfers much of the plasma thermal energy into kinetic energy

of a liner which is accelerated by ablation. Since the power density associated with the plasma is one to two orders-of-magnitude larger than with high explosive or magnetic drivers, much larger implosion velocities are possible. Disadvantages associated with ohmic heating and magnetic field diffusion are overcome. It is also possible to drive spherical liners. The single shot character of the prior art concept is overcome by beam propagation to a small replaceable gas filled container which encloses the liner.

A third class of device utilizes the explosive plasma to drive a fast liner through heat conduction, which in turn drives a structured microsphere. As the liner implodes, its kinetic energy is converted into a concentrated, intense plasma which implodes the structured microsphere through a combination of ablation and velocity multiplication. Alternatively, the interior of a spherical liner could be evacuated with the pellet supported by a thin film.

By converting from thermal energy to kinetic energy and back to thermal energy, the energy delivered to the microsphere is shaped in time and greatly intensified relative to the initial 10^{17} - 10^{20} cm^{-3} plasma. Thus, rather than trying to develop a new technology with sufficient power levels for implosion, the preceding concept utilizes present or near term technology.

Compared with lasers and low-impedance, low-voltage electron beams, the energy on target would be much larger and with similar power levels. Equally important, the energy delivered to the microsphere is naturally pulse shaped, thus allowing for shock overtaking and larger ion temperatures in the core of the microsphere. Thus, the fast liner implosion of a structure microsphere is low cost and offers short-term payoff, relative to the prior art.

Finally, the entire liner and pellet combination is enclosed in a small replaceable container which may ultimately prove to be advantageous from a power reactor design standpoint.

ACKNOWLEDGMENT

The author gratefully acknowledges B. B. Godfrey and W. P. Gula for informative discussions. I also acknowledge B. B. Godfrey for his development of the most advanced particle-in-cell numerical simulation code in existence. The CCUBE code has provided confirmation for the basic nonlinear analytical models and insight into the time-dependent evolution of the streaming instabilities. The author is indebted to C. Clark and C. Ekdahl for numerous discussions of their experimental results.

REFERENCES

1. L. E. Thode and R. N. Sudan, "Two-Stream Instability Heating of Plasma by Relativistic Electron Beams," Phys. Rev. Lett. 30, 732 (1973).

2. B. B. Godfrey, W. R. Shanahan, and L. E. Thode, "Linear Theory of a Cold Relativistic Beam Propagating Along an External Magnetic Field," Phys. Fluids, 18, 346 (1975).

3. L. E. Thode and R. N. Sudan, "Plasma Heating by Relativistic Electron Beams. I. Two-Stream Instability," Phys. Fluids 19, 1552 (1975).

4. L. E. Thode and R. N. Sudan, "Plasma Heating by Relativistic Electron Beams. II. Return Current Interaction," Phys. Fluids 18, 1564 (1975).

5. L. E. Thode, "Energy Lost by a Relativistic Electron Beam Due to Two-Stream Instability," Phys. Fluids 19, 305 (1976).

6. L. E. Thode and B. B. Godfrey, "Energy Lost by a Relativistic Electron Beam Propagating Along an External Magnetic Field," Phys. Fluids 19, 316 (1976).

7. L. E. Thode, "Plasma Heating by Scattered Relativistic Electron Beams: Correlations Among Experiment, Simulation, and Theory," Phys. Fluids 19, 831 (1976); see references for plasma heating experiments prior to 1975.

8. J. Benford, V. Bailey, T. S. T. Young, D. Dakin, B. Ecker, S. Putnam, M. Di Capua, and R. Cooper (Physics International Company); D. A. Hammer, K. Gerber, K. R. Chu, and R. Clark (Naval Research Laboratory); M. Greenspan, J. Sethian, C. Ekdahl, and C. Wharton (Cornell University); L. Thode (Los Alamos Scientific Laboratory), "Progress Toward Relativistic Electron Beam Heating of Magnetically Confined Systems," Sixth International Conference on Plasma and Controlled Nuclear Fusion Research (Berchtesgaden, FRG, 1976).

9. L. E. Thode, "Effect of Electron-Ion Collisions on the Nonlinear State of the Relativistic Two-Stream Instability," Phys. Fluids 20, 2121 (1977); see references for plasma heating experiments from 1975 through 1977.

10. R. J. Briggs, J. C. Clark, T. J. Fessenden, R. E. Hester, and E. J. Lauer, "Transport of Self-Focused Relativistic Electron Beams," Proceedings of the 2nd International Topical Conference on High Power Electron and Ion Beam Research and Technology (Ithaca, New York, 1977); Vol. I, 319.

11. A. K. L. Dymoke-Bradshaw, A. E. Dangor, D. A. Hammer, and J. D. Kilkenny, "Plasma Heating by Injection of Relativistic Electron Beam in Neutral Gas," Proceedings of the 2nd International Topical Conference on High Power Electron and Ion Beam Research and Technology (Ithaca, New York, 1977); Vol. I, 343.

12. B. Jurgens, P. H. deHaan, E. H. A. Granneman, and H. J. Hopman, "Measurements on the Energy Loss of a Relativistic Electron Beam in a Plasma," Proceedings of the 2nd International Topical Conference on High Power Electron and Ion Beam Research and Technology (Ithaca, New York, 1977); Vol. I, 369.

13. C. B. Wharton, "Effects of E-Beam Temperature on Plasma Heating," Proceedings of the 2nd International Topical Conference on High Power Electron and Ion Beam Research and Technology (Ithaca, New York, 1977); Vol. I, 407.

14. R. V. Lovelace and R. N. Sudan, "Plasma Heating by High-Current Relativistic Electron Beams," Phys. Rev. Lett. 27, 1256 (1971).

15. Ya. B. Fainberg, V. D. Shapiro, and V. I. Shevchenko, "Nonlinear Theory of Interaction Between a Monochromatic Beam of Relativistic Electrons and Plasma," Zh. Eksp. Theor. Fiz. 57, 966 (1969) [Sov. Phys. - JETP 30, 528 (1970)].

16. L. I. Rudakov, "Collective Slowing Down of an Intense Beam of Relativistic Electrons in a Dense Plasma Target," Zh. Eksp. Teor. Fiz. 59, 2091 (1970) [Sov. Phys. - JETP 32, 1134 (1971)].

17. R. I. Kovtun and A. A. Rukhadze, "Nonlinear Interaction of a Low-Density Relativistic Electron Beam with a Plasma," Zh. Eksp. Teor. Fiz. 58, 1709 (1970) [Sov. Phys. - JETP 31, 915 (1970)].

18. B. N. Breizman and D. D. Ryutov, "Quasilinear Relaxation of an Ultrarelativistic Electron Beam in a Plasma," Zh. Eksp. Teor. Fiz. 60, 408 (1971) [Sov. Phys. - JETP 33, 220 (1971)].

19. A. A. Rukhadze and V. G. Rukhlin, "Injection of a Relativistic Electron Beam into a Plasma," Zh. Eksp. Teor. Fiz. 61, 177 (1971) [Sov. Phys. - JETP 34, 93 (1972)].

20. V. B. Krasovitskii, "Nonlinear Theory of Interaction Between a Bounded Relativistic Beam and a Plasma," Zh. Eksp. Theor. Fiz. 62, 995 (1972) [Sov. Phys. - JETP 35, 525 (1972)].

21. B. N. Breizman, D. D. Ryutov, and P. Z. Chebotaev, "Nonlinear Effects in the Interaction Between an Ultrarelativistic Electron Beam and a Plasma," Zh. Eksp. Teor. Fiz. 62, 1409 (1972) [Sov. Phys. - JETP 35, 741 (1972)].

22. N. G. Matsiborko, I. N. Onishchenko, V. D. Shapiro, and V. I. Shevchenko, "A Non-Linear Theory of Instability of a Mono-Energetic Electron Beam in Plasma," Plasma Phys. 14, 591 (1972).

23. V. B. Krasovitskii, "On the Nonlinear Theory of the Beam-Plasma Instability," Zh. Eksp. Teor. Fiz. 64 1597 (1973) [Sov. Phys. - JETP 37, 809 (1973)].

24. A. J. Toepfer and J. W. Poukey, "Saturation of the Relativistic Beam-Plasma Instability for Arbitrary Density Ratios," Phys. Lett. A42, 383 (1973).

25. G. Benford, "Radiation and Ionization by Relativistic Electron Beams," J. Plasma Phys. 10, 203 (1973).

26. A. J. Toepfer and J. W. Poukey, "Nonlinear Saturation of the Relativistic Beam-Plasma Instability in the Presence of Ion Density Fluctuations," Phys. Fluids 16, 1546 (1973).

27. L. E. Thode, "Plasma Heating by Intense Relativistic Electron Beam Due to Two-Stream and Return-Current Interactions," Ph.D. Thesis, Cornell University (1974).

28. L. E. Thode and B. B. Godfrey, "Energy Lost by a Relativistic Electron Beam Due to Two-Stream Instability," in the Conference Record of the IEEE Second International Conference on Plasma Science (Ann Arbor, Michigan, 1975), 55.

29. C. Ekdahl, M. Greenspan, J. Sethian, and C. B. Wharton, "Observation of Enhancement of Plasma Heating with Relativistic Electron Beams Resulting from a Reduction of Anode Foil Scattering," Bull. Am. Phys. Soc. 20, 1270 (1975).

30. C. Ekdahl and J. Sethian, "Beam Temperature Effects on the Relativistic Two-Stream Heating of Plasma," to be submitted to Phys. Rev. Lett.

31. L. Thode, "Relativistic Streaming Instability Enhanced by Judicious Choice of External Magnetic Field Strength," in the Conference Record of 1978 IEEE International Conference on Plasma Science (Monterey, California, 1978), 284.

32. J. Sethian, "Thompson Scattering and Diamagnetic Loop Studies of a Relativistic Electron Beam-Heated Plasma," Ph.D. Thesis, Cornell University (1976).

33. M. Greenspan, "Plasma Heating by a Relativistic Electron Beam: An Experimental Study," Ph.D. Thesis, Cornell University (1976).

34. C. Ekdahl, Los Alamos Scientific Laboratory, private communication, March 1978.

35. C. Ekdahl, Los Alamos Scientific Laboratory, private communication, August, 1978.

36. L. E. Thode, "Preliminary Investigation of Anomalous Relativistic Electron Beam into a 10^{17} to 10^{20} cm^{-3} Density Plasma," Los Alamos Scientific Laboratory report, LA-7215-MS (April 1978).

37. I. Smith, "Liquid Dielectric Pulse Line Technology," in Energy Storage, Compression, and Switching, edited by W. H. Bostick, V. Nardi, and O. S. F. Zucker (Plenum Press, New York, 1976), 3.

38. A. I. Pavlovskii, V. S. Bosamykin, G. D. Kuleshov, A. I. Gerasimov, V. A. Tananakin, and A. P. Klement'ev, "Multielement Accelerators Based on Radial Lines," Dokl. Akad. Nauk. SSSR 222, 817 (1975) [Sov. Phys. - Dokl. 20, 441 (1975)].

39. V. I. Kazacha and I. V. Kozhukhov, "Use of Radial Transmission Lines in Pulsed Accelerators," Zh. Tekh. Fiz. 46, 1477 (1976) [Sov. Phys. - Tech. Phys. 21, 841 (1976)].

40. L. E. Thode, "Design Considerations for Air Force Weapons Laboratory FX25 Plasma Heating Experiment," Los Alamos Scientific Laboratory report LA-7233-MS (April 1978).

41. C. Clark, Air Force Weapons Laboratory, private communication, March 1978.

42. J. Benford, Physics International Company, private communiation, September 1975.

43. M. E. Jones and L. E. Thode, "A Study of Relativistic Electron Beams Generated by a Foilless Diode," Los Alamos Scientific Laboratory report LA-7600-MS (January 1979).

44. S. Humphries, "Intense Ion Beam Acceleration and Transport," Proceedings of the 2nd International Topical Conference on High Power Electron and Ion Beam Research and Technology (Ithaca, New York, 1977); Vol. I., 83.

45. C. M. Fowler, R. S. Caird, and W. B. Garn, "An Introduction to Explosive Magnetic Flux Compression Generators," Los Alamos Scientific Laboratory report LA-5890-MS (March 1975).

46. H. W. Greene, D. Holder, D. Mathews, J. Knaur, and G. L. Brown, "Feasibility Study for a Threat-Environment Electromagnetic Pulse Field Simulation System," U. S. Army Missile Command Technical Report RG-76-63 (June 1976).

47. Niccia Grant Cooper, compiler, "Theoretical Division Annual Report July 1975 - September 1976," Los Alamos Scientific Laboratory report LA-6816-PR (1976), p. 148. CCUBE was designed and implemented by B. B. Godfrey.

48. H. R. Jory and A. W. Trivelpiece, "Exact Relativistic Solution for the One-Dimensional Diode," J. Appl. Phys. 40, 3924 (1969).

49. C. Ekdahl, Los Alamos Scientific Laboratory, private communication, April 1978.

50. S. A. Goldstein, G. Cooperstein, R. Lee, D. Mosher, and S. J. Stephanakis, "Focusing of Intense Ion Beams from Pinched-Beam Diodes," Phys. Rev. Lett. 40, 1504 (1978).

51. J. A. Pasour, R. A. Mahaffey, J. Golden, and C. A. Kapetanakos, "Reflex Tetrode with Unidirectional Ion Flow," in the Conference Record of the 1978 IEEE International Conference on Plasma Science (Monterey, California, 1978), 107.

52. R. A. Mahaffey, J. A. Pasour, J. Golden, and C. A. Kapetanakos, "Studies of Efficient Ion Beam Generation with Reflex Tetrodes," in the Conference Record of the 1978 IEEE International Conference on Plasma Science (Monterey, California, 1978), 108.

53. D. J. Johnson, G. W. Kuswa, R. J. Leeper, S. Humphries, and G. R. Hadley, "Initial Studies of a Magnetically Insulated Ion Diode," in the Conference Record of the 1978 IEEE International Conference on Plasma Science (Monterey, California, 1978), 175.

54. M. Greenspan, D. Hammer, and R. N. Sudan, "A Spherically Focusing Magnetically Insulated Ion Diode," in the Conference Record of the 1978 IEEE International Conference on Plasma Science (Monterey, California, 1978), 176.

55. W. I. Linlor, "Plasma-Target Fusion Machine," Hughes Aircraft Company Research report 128 (October, 1959).

56. J. G. Linhart, H. Knoepfel, and C. Goorlan, "Amplification of Magnetic Fields and Heating of Plasma by a Collapsing Metallic Shell," Nucl. Fusion Suppl., part 2, p. 733 (1962).

57. A. R. Sherwood, B. L. Freeman, R. A. Gerwin, T. R. Jarboe, R. A. Krakowski, R. C. Malone, J. Marshall, R. L. Miller, B. Suydam, R. L. Hagenson, E. L. Kemp, R. W. Moses, and C. E. Swannack, "Fast Liner Proposal," Los Alamos Scientific Laboratory report LA-6707-P (August 1977).

58. P. J. Turchi and W. L. Baker, "Generation of High-Energy Plasmas by Electromagnetic Implosion," J. Appl. Phys. 44, 4936 (1973).

59. R. J. Mason and R. L. Morse, "Hydrodynamics and Burn of Optimally Imploded Deuterium-Tritium Spheres," Phys. Fluids 18, 814 (1975).

60. S. D. Bertke and E. B. Goldman, "The Dynamics of High Compression of Laser Fusion Targets," Nucl. Fusion 18, 509 (1978).

61. R. J. Mason, "Performance of Structured Laser Fusion Pellets," Los Alamos Scientific Laboratory report LA-5898-MS (October, 1975).

62. G. S. Fraley, E. J. Linnebur, R. J. Mason, and R. L. Morse, "Thermonuclear Burn Characteristics of Compressed Deuterium-Tritium Microspheres," Phys. Fluids 17, 474 (1974).

63. J. E. Hammel, Los Alamos Scientific Laboratory, private communication (September 1977).

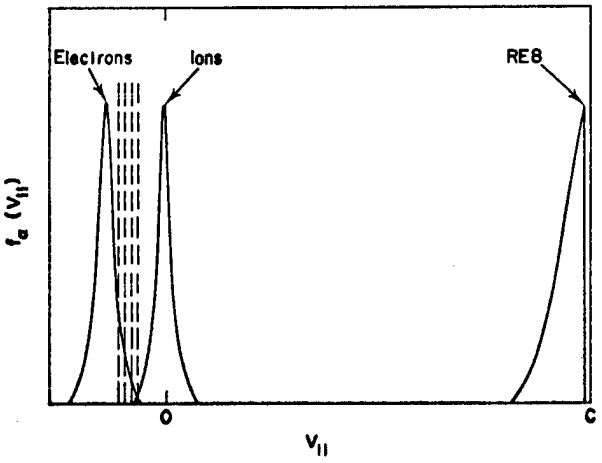

Fig. 1. Characteristic relationship between the beam and plasma species for resistive heating. The component of velocity along the direction of beam propagation is $v_{||}$. Anomalous resistance results from the generation of low frequency waves, which are indicated by the dashed lines.

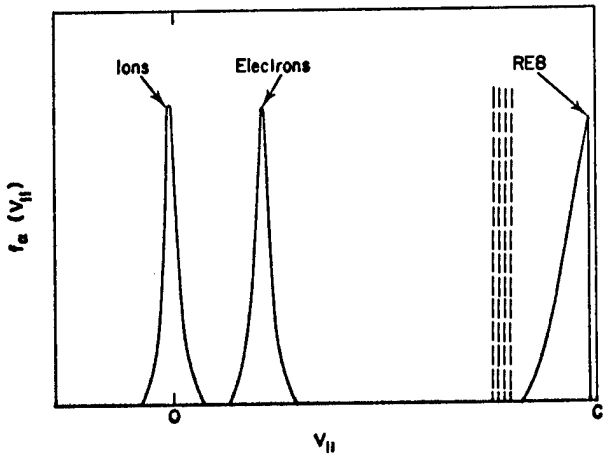

Fig. 2. Characteristic relationship between the beam and plasma species for relaxation heating. The component of velocity along the direction of beam propagation is $v_{||}$. Generation of high frequency waves, indicated by dashed lines, removes energy from the beam.

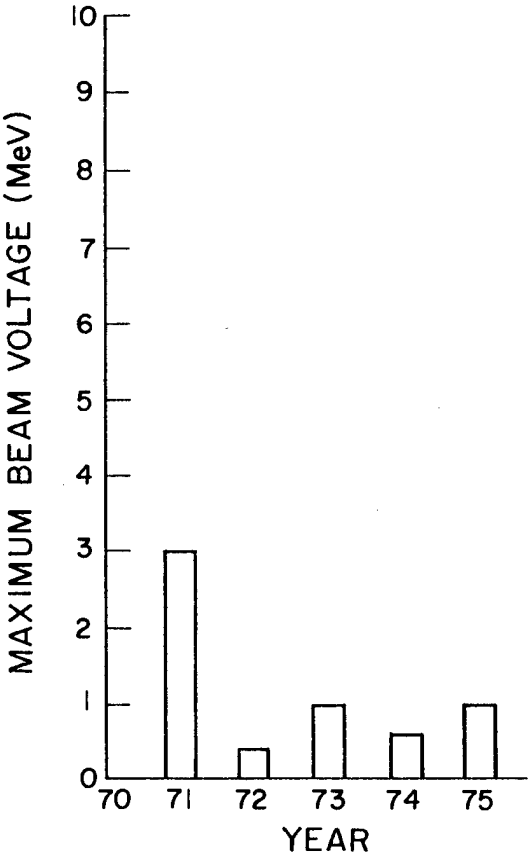

Fig. 3. Maximum experimental relativistic electron beam voltages utilized from 1970 to 1975. The trend is toward lower voltage beams.

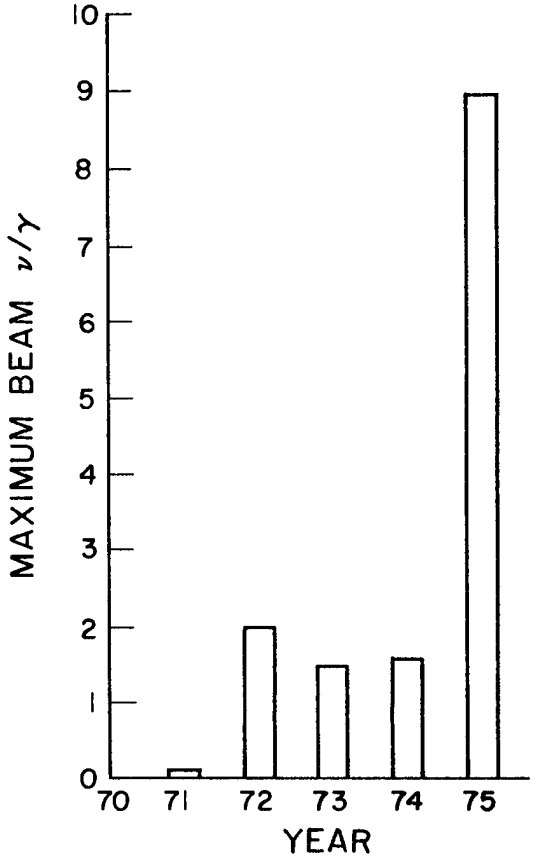

Fig. 4. Maximum experimental relativistic electron beam v/γ utilized from 1970 to 1975. The trend is toward higher v/γ beams.

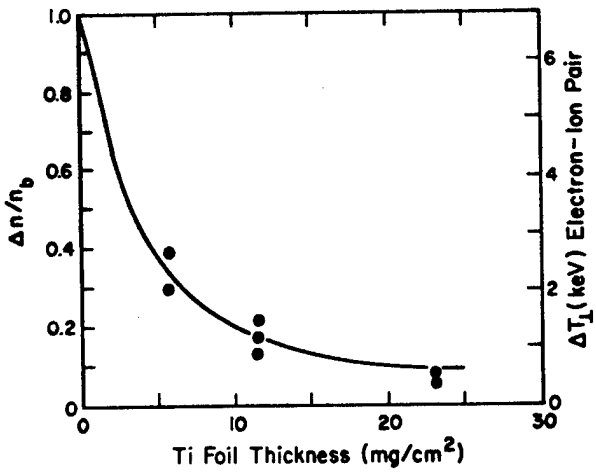

Fig. 5. Ekdahl et al. experiment.[29] Data measured with diagmagnetic loops as a function of anode foil thickness. Solid line is $\Delta n/n_b$ for 350 keV beam and a beam-to-plasma particle density ratio of 2.8×10^{-3}. Anode foil scattering is negligible when the quantity $\Delta n/n_b \cong 1$.

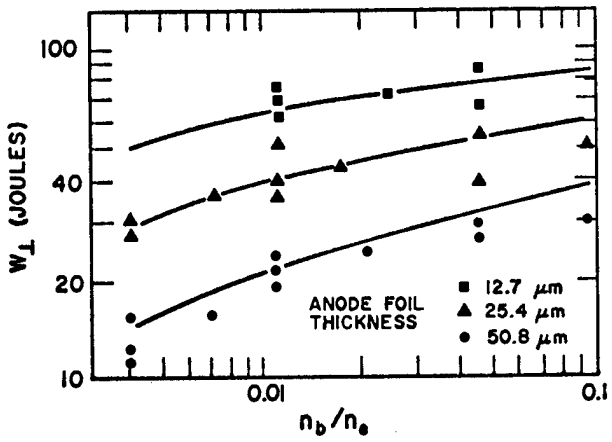

Fig. 6. Ekdahl and Sethian experiment.[30] Scaling of plasma heating with beam-to-plasma particle density ratio n_b/n_e and anode foil thickness. Data is plasma perpendicular energy as determined by a diamagnetic loop. Theoretical predictions are indicated by the solid curves.

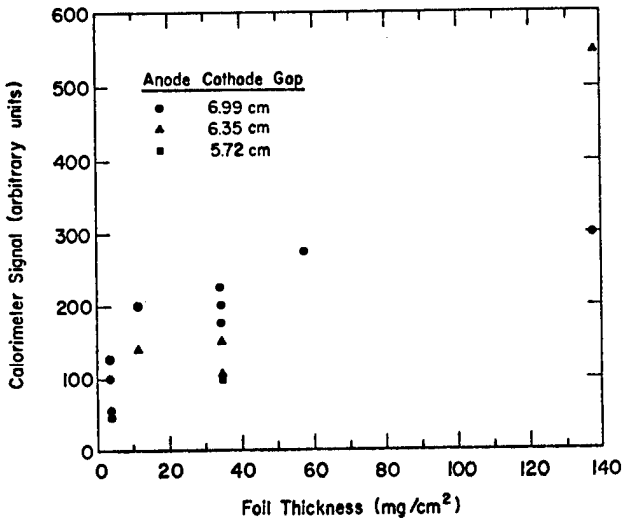

Fig. 7. Clark propagation experiment.[40] Beam energy transmitted to a calorimeter as a function of anode-cathode gap spacing and anode foil thickness. The overall trend is a reduction in transmisson for reduced anode foil thickness. For the 25.4 μm and 76.2 μm Ti foils, the trend is a reduction in transmission for reduced anode-cathode gap.

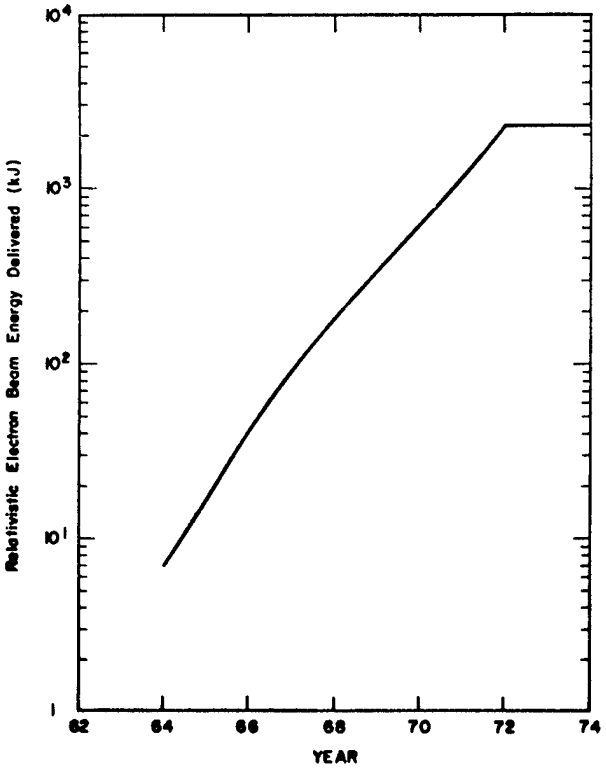

Fig. 8. Historical development of high impedance generator technology.[42]

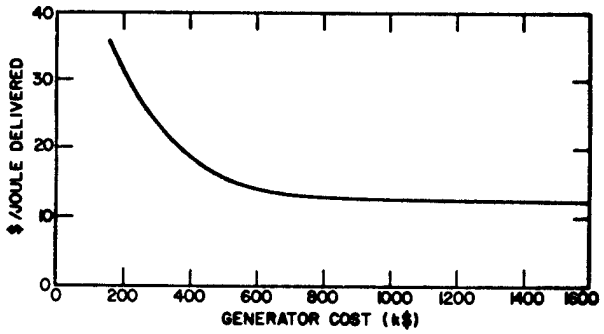

Fig. 10. Approximate cost per joule delivered as a function total generator cost.

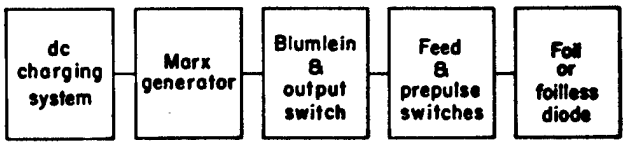

Fig. 11. Five basic components of a high impedance relativistic electron beam generator.

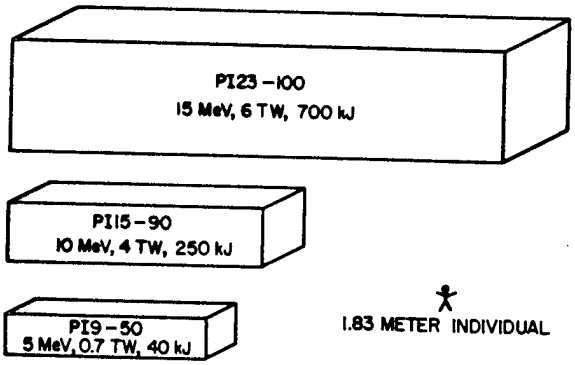

Fig. 9. Approximate size of PI23-100, PI15-90, and PI9-50 generators relative to a 1.83 meter individual.

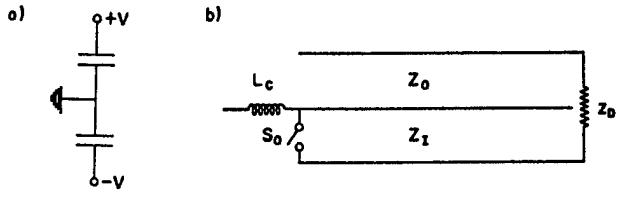

Fig. 12. a) Electrical equivalent of a Marx stage. b) Electrical equivalent of a Blumlein and diode.

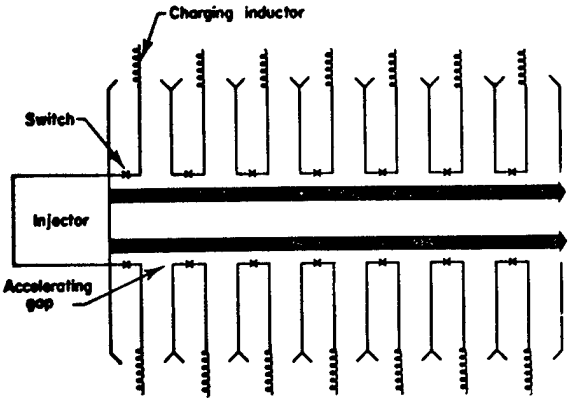

Fig. 13. Conceptual diagram of the radial pulse line accelerator.

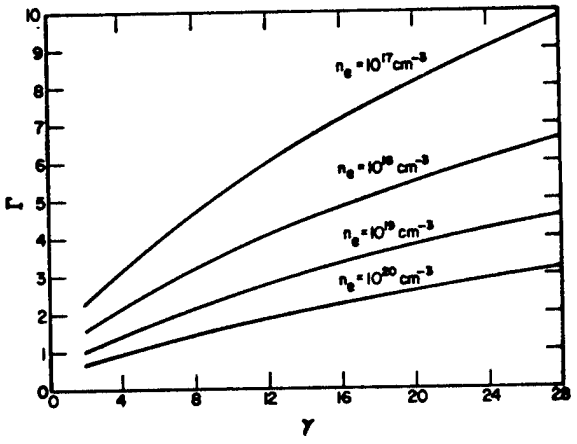

Fig. 14. Dimensionless parameter Γ as a function of the relativistic factor γ for given values of the plasma electron density.

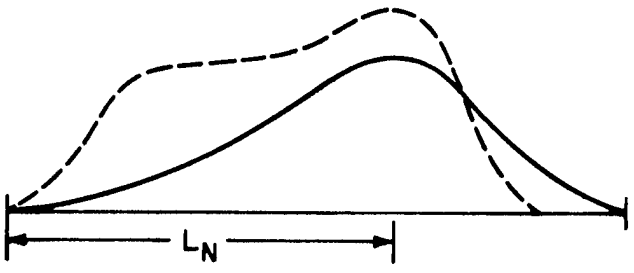

Fig. 15. Characteristic nonuniform energy deposition along the direction of beam propagation associated with the streaming instabilities. A one-dimensional interaction is represented by the solid line. The dashed line represents a two-dimensional interaction.

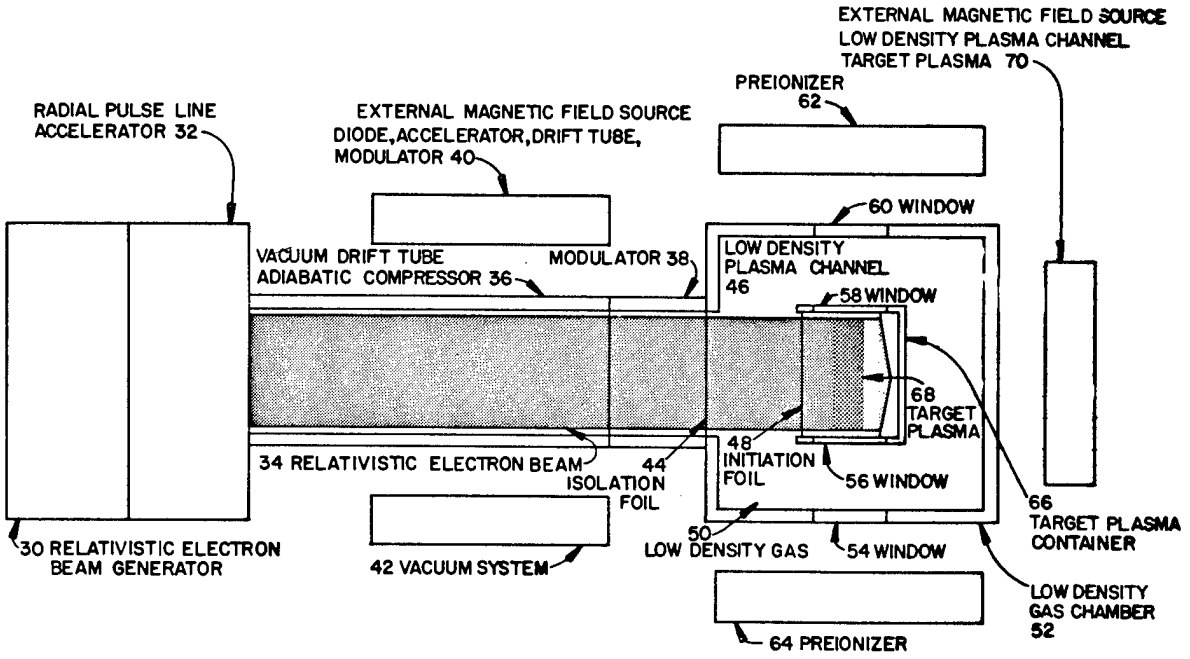

Fig. 16. Conceptual diagram illustrating the major components of a system which uses the high-energy density plasma as a direct source for x-rays or neutrons.

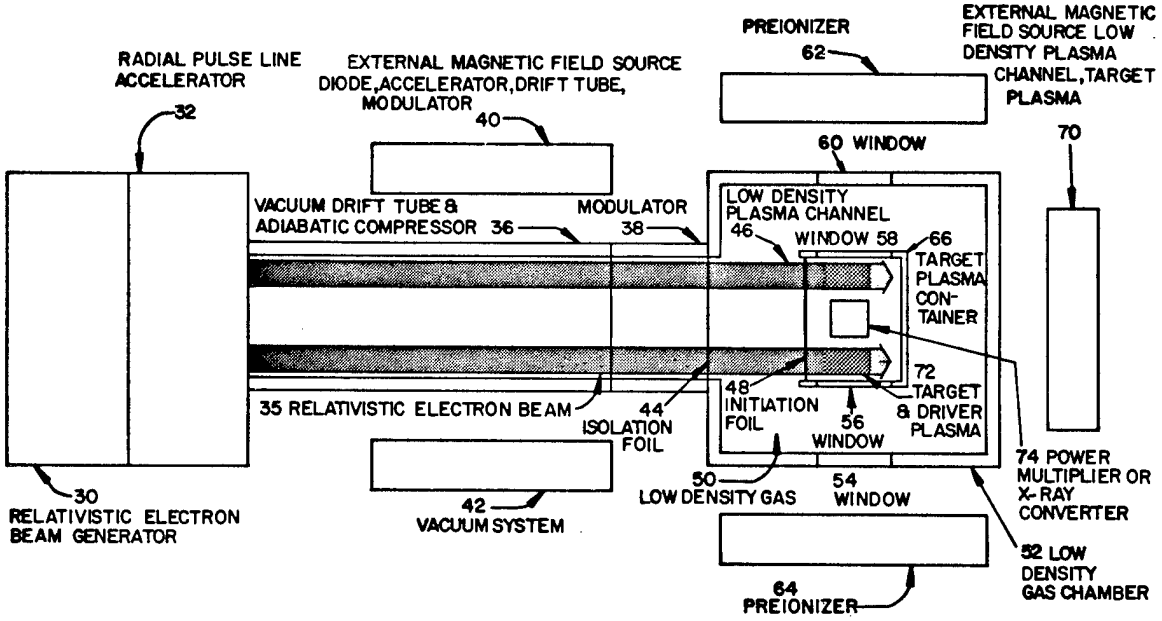

Fig. 17. Conceptual diagram illustrating the major components of a system which uses the high-energy density plasma to drive power multiplication or x-ray conversion devices.

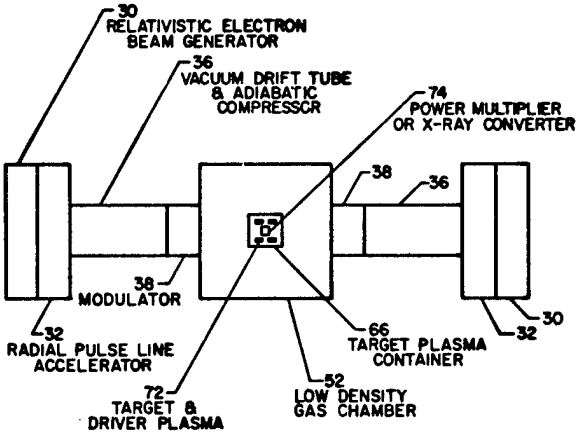

Fig. 18. Simplified conceptual diagram of a two annular beam system. Regions of energy deposition do not overlap.

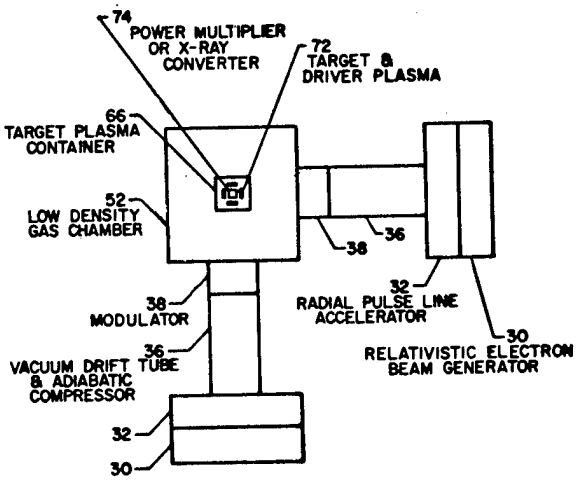

Fig. 19. Simplified conceptual diagram of a two annular beam system providing improved spherical symmetry. Regions of energy deposition do not overlap.

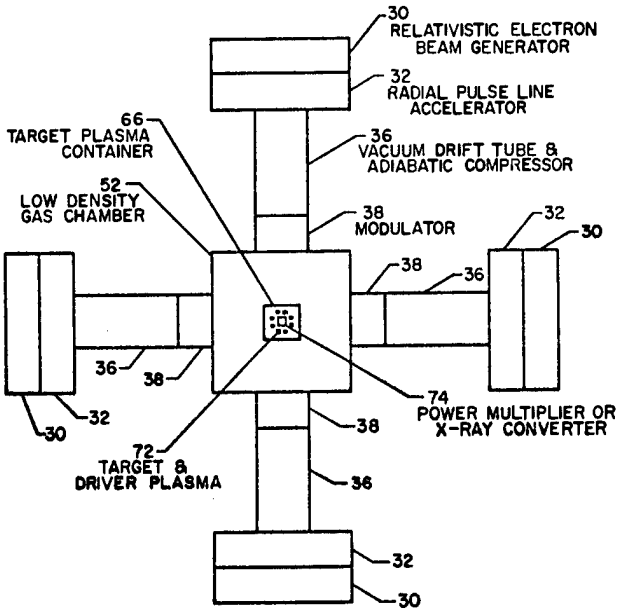

Fig. 20. Simplified conceptual diagram of a four annular beam system providing spherical symmetry in a multi-megajoule system. Regions of energy deposition do not overlap.

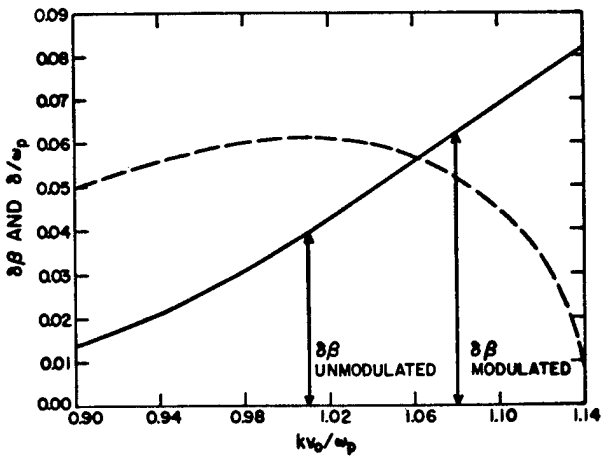

Fig. 21. Characteristic growth rate δ/ω_p (dashed line) and velocity change $\delta\beta$ (solid line) as a function of wavenumber k for the streaming instabilities.

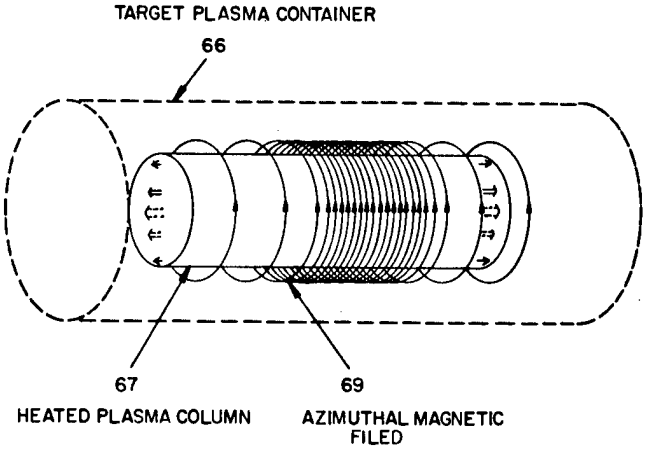

Fig. 22. Configuration of anomalous pinch. The plasma target container 66 is represented by the dashed lines. Heat conduction loss occurs predominately along the axis of the heated cylinder of plasma.

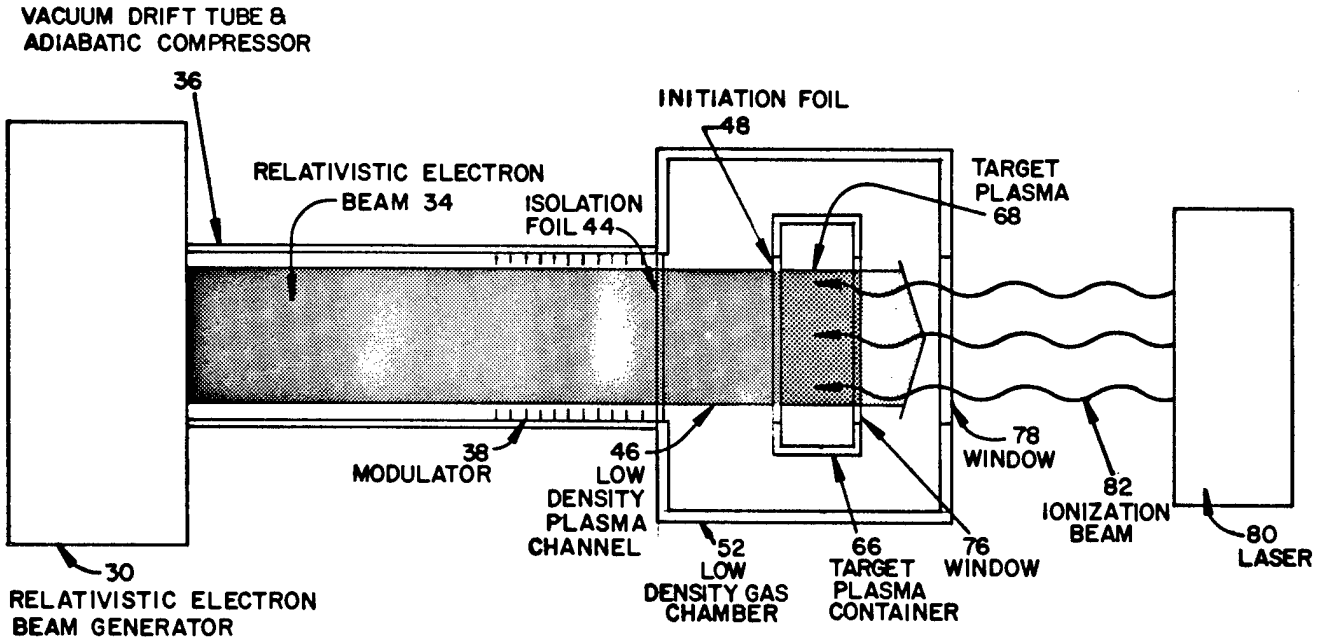

Fig. 23. Schematic illustration of the anomalous pinch using a single laser preionizer.

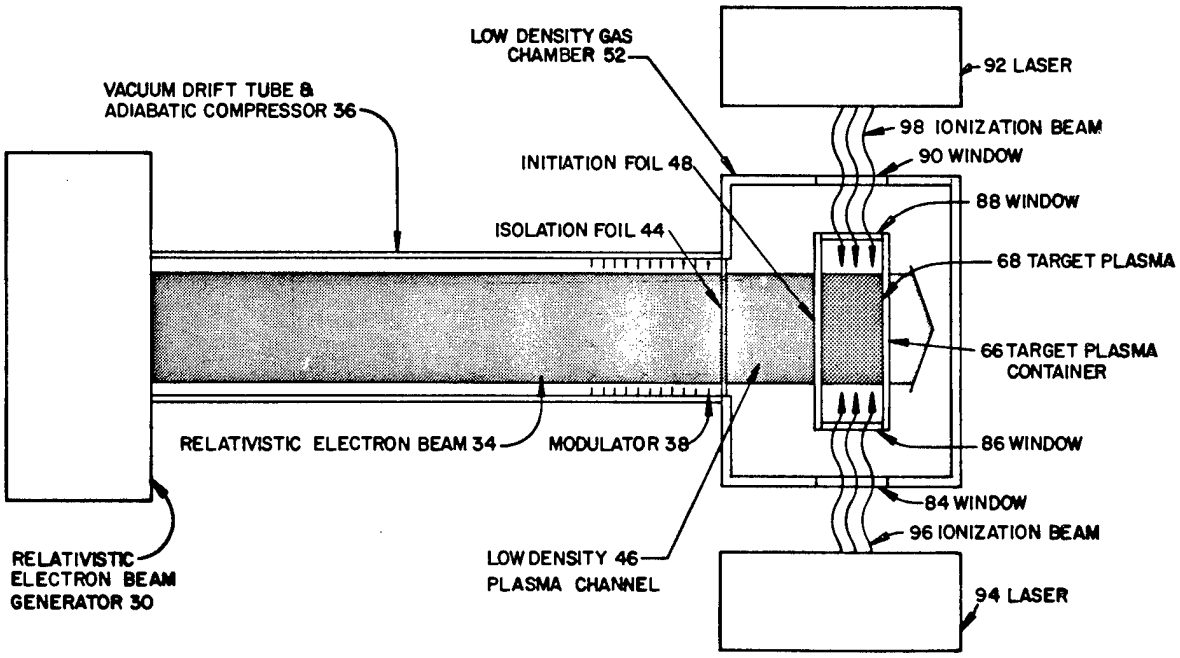

Fig. 24. Schematic illustration of the anomalous pinch using a two laser preionizer.

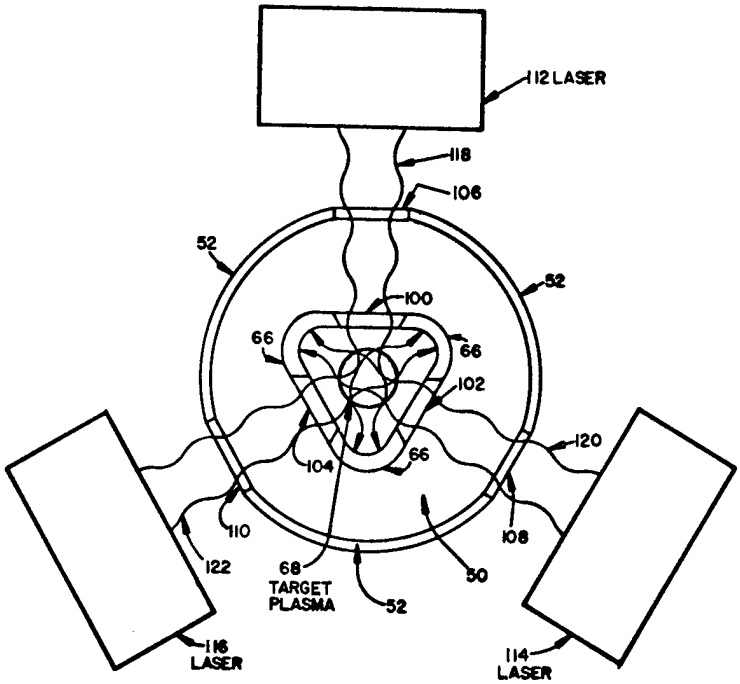

Fig. 25. End view of the anomalous pinch using three laser preionizers.

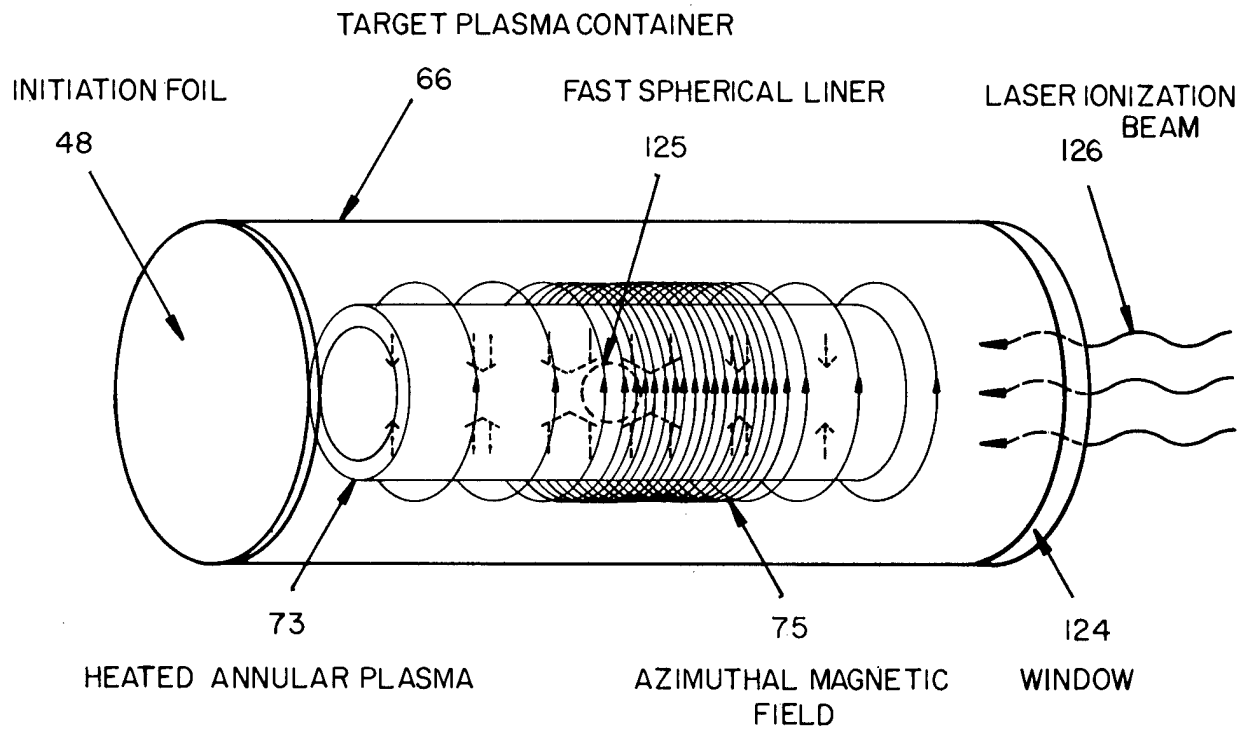

Fig. 26. Basic geometry for driving a fast spherical liner. Dashed arrows indicate the direction and magnitude of the heat flow.

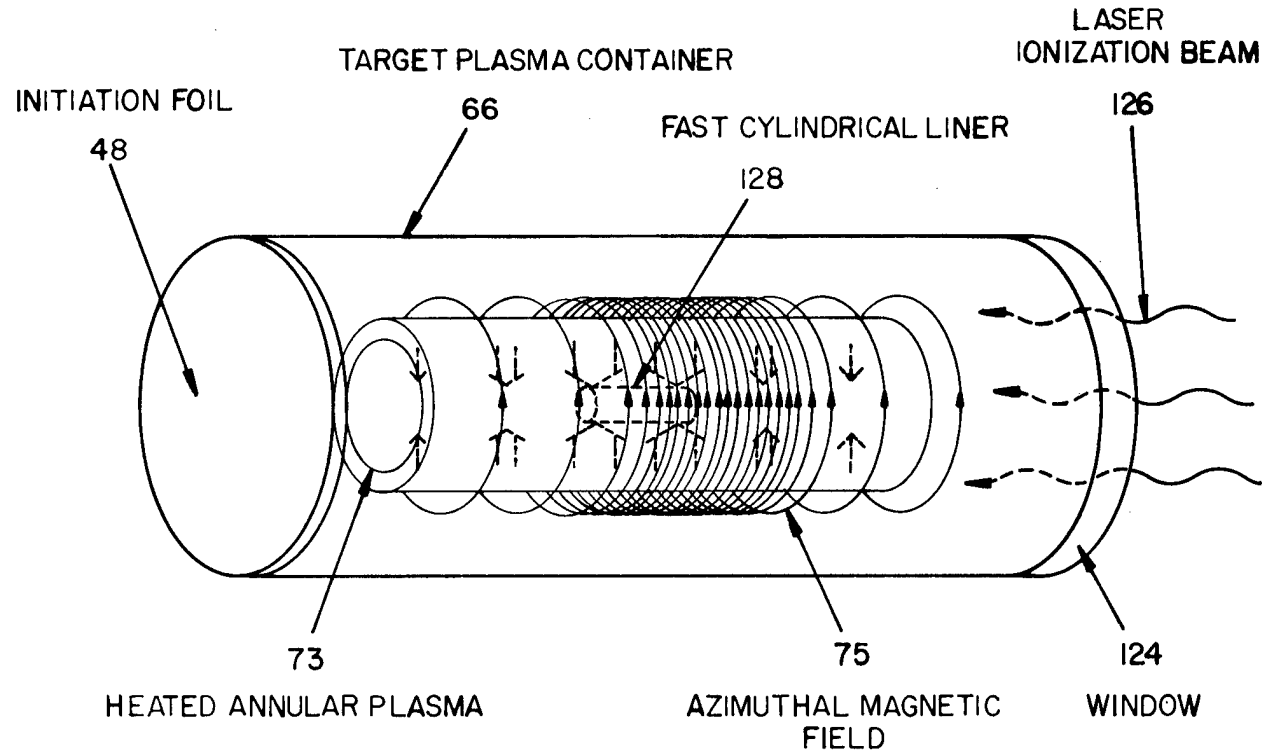

Fig. 27. Basic geometry for driving a fast cylindrical liner. Dashed arrows indicate the direction and magnitude of the heat flow.

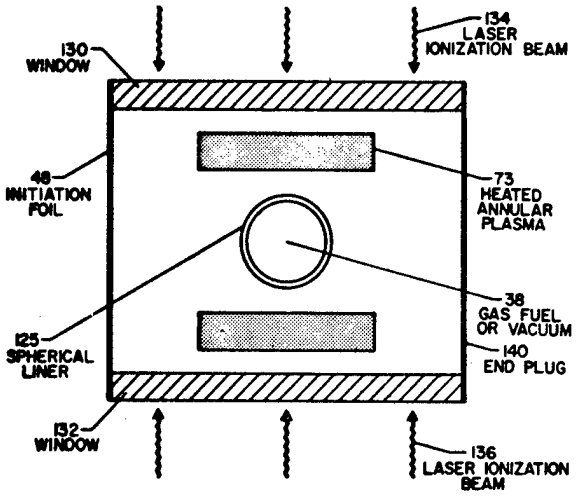

Fig. 28. Cross-sectional view of spherical liner configuration, with dual ionization beams.

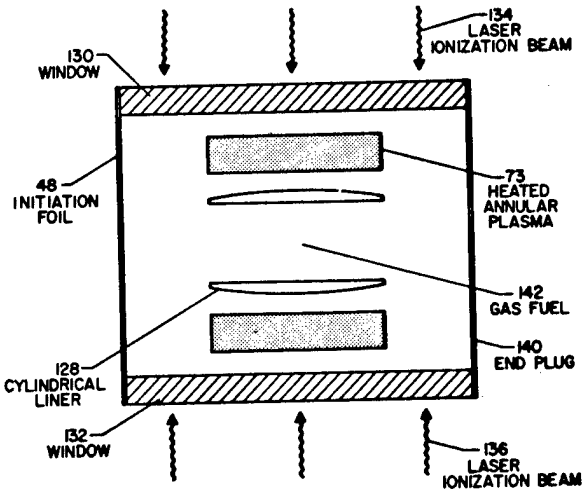

Fig. 29. Cross-sectional view of cylindrical liner configurations with dual ionization beams.

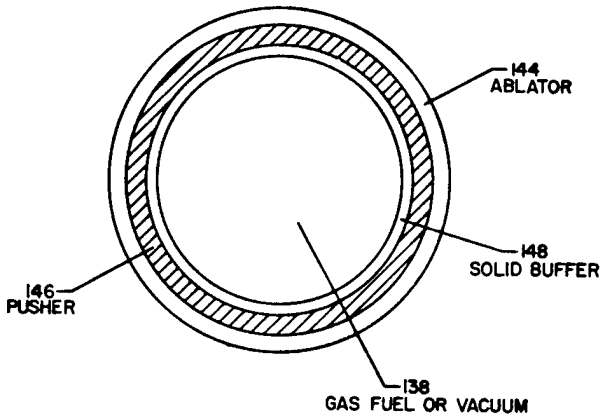

Fig. 30. Detail of fast spherical liner.

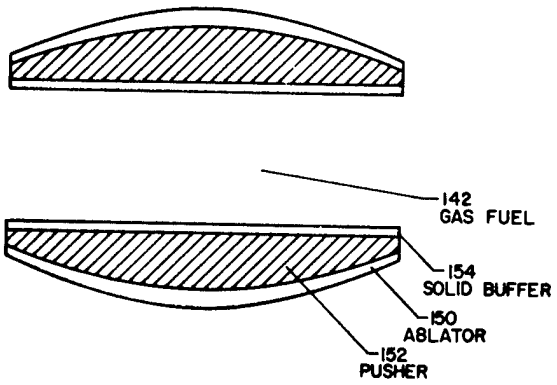

Fig. 31. Detail of fast cylindrical liner.

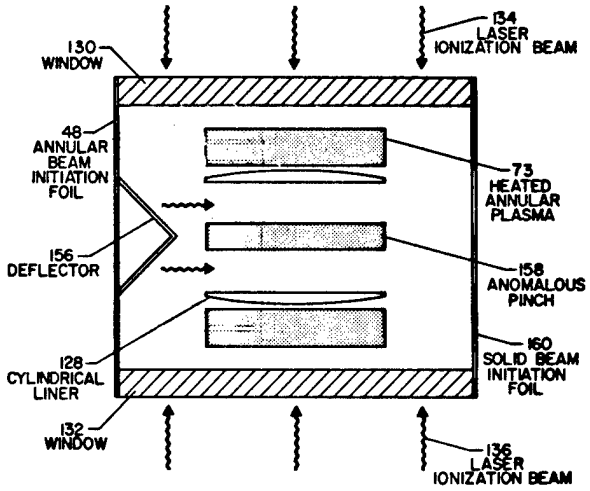

Fig. 32. Configuration similar to LASL CTR Division's fast liner[55] concept.

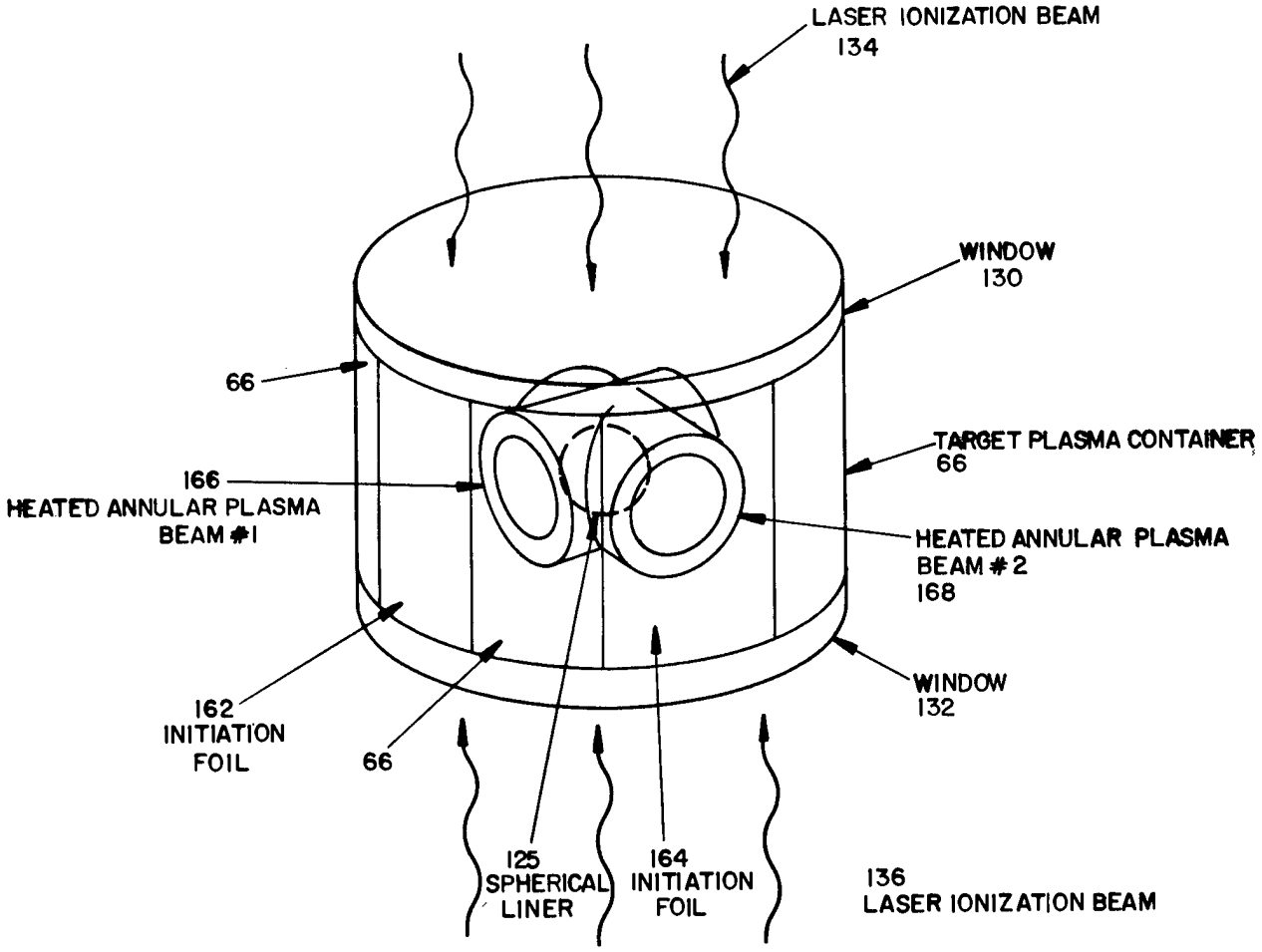

Fig. 33. Configuration using two relativistic electron beams to drive a fast spherical liner.

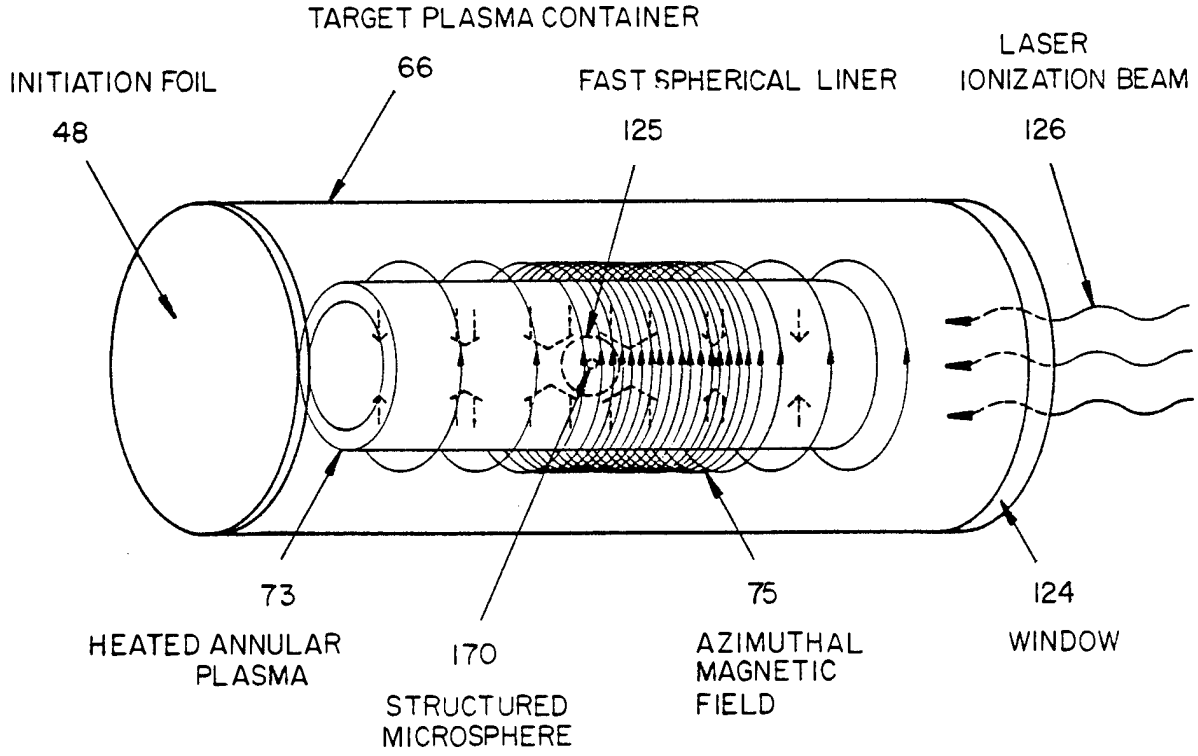

Fig. 34. Basic geometry for fast spherical liner implosion of a structured microsphere. Dashed arrows indicate direction and magnitude of heat flow.

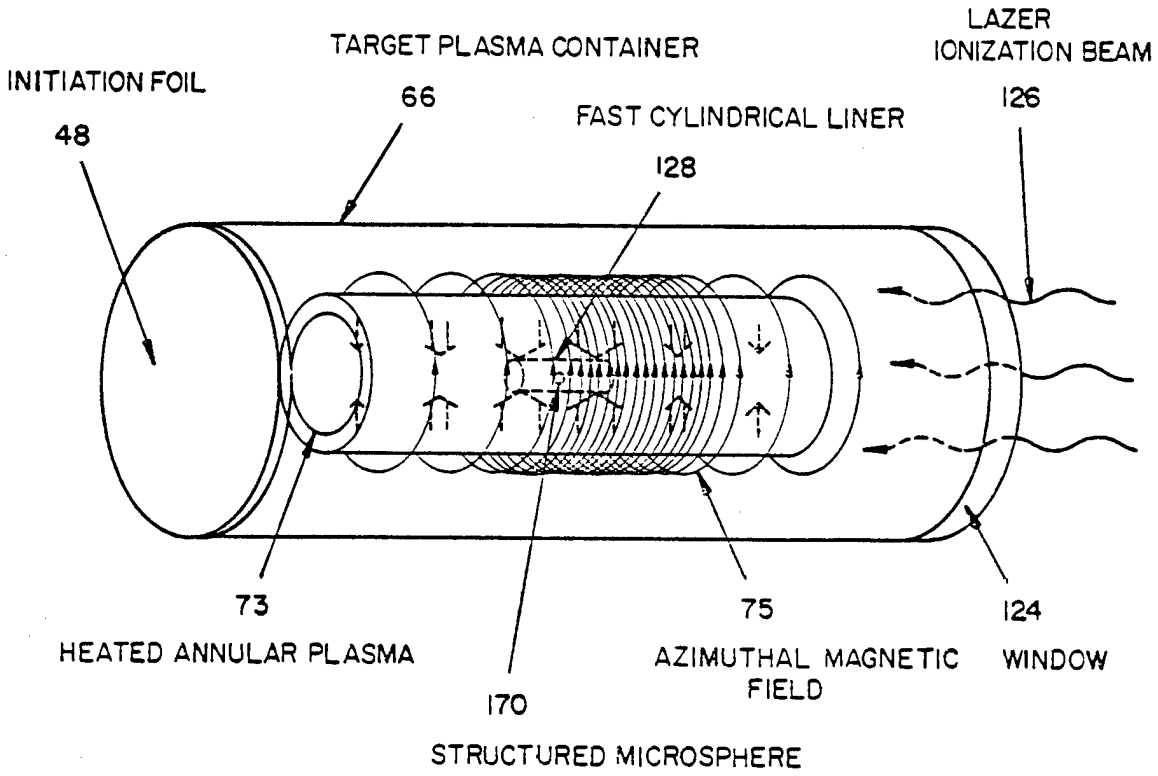

Fig. 35. Basic geometry for fast cylindrical liner implosion of a structured microsphere. Dashed arrows indicate direction and magnitude of heat flow.

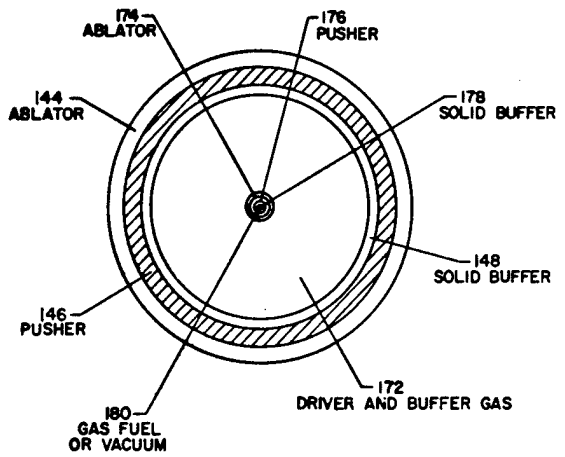

Fig. 36. Detail of fast spherical liner and structured microsphere.

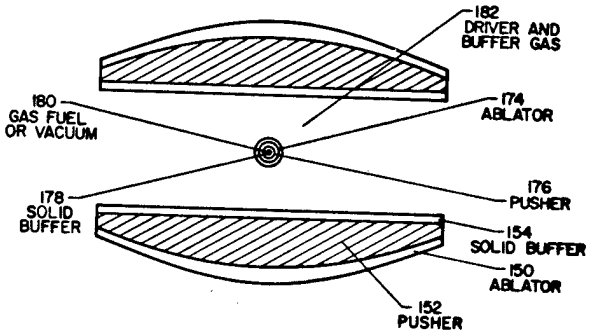

Fig. 37. Detail of fast cylindrical liner and structured microsphere.

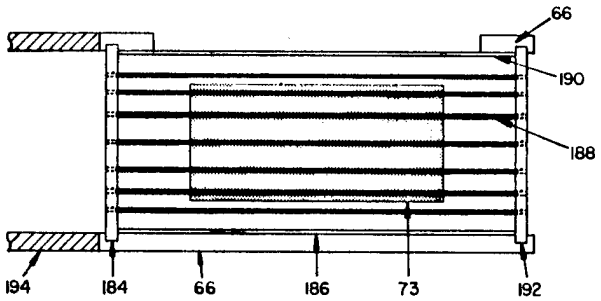

38. Cross-sectional view of a wire array device for x-ray generation.

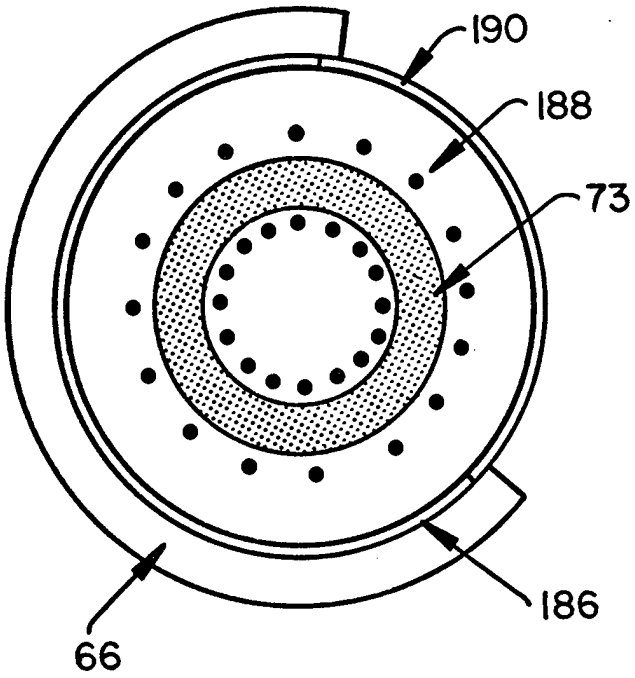

Fig. 39. End view of a wire array device for x-ray generation.

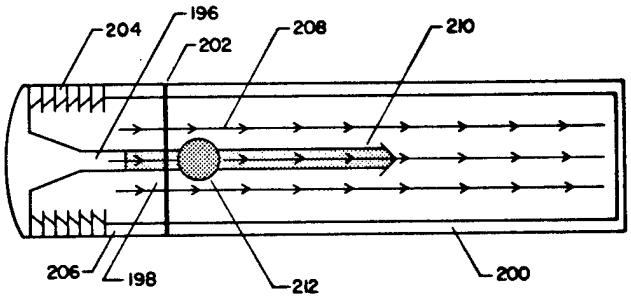

Fig. 40. Typical configuration of a prior art relativistic electron beam-plasma heating experiment.

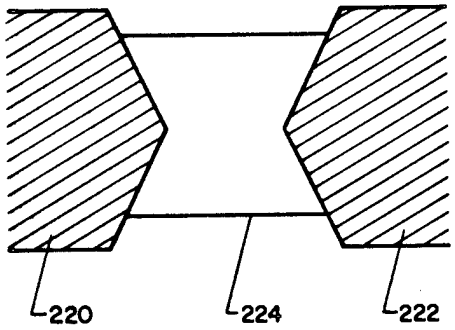

Fig. 41. Typical configuration of a prior art cylindrical liner.

☆ U.S. Government Printing Office: 1980 — 677 — 115/56